Identification of novel PfEMP1 variants containing domain cassettes 11, 15 and 8 that mediate the *Plasmodium falciparum* virulence-associated rosetting phenotype

Florence McLean[1*], Brian R. Omondi[1*], Nouhoum Diallo[1], Stanley Otoboh[1], Carol Kifude[1], Abdirahman Abdi[2], Rivka Lim[1], Thomas Otto[3], Ashfaq Ghumra[1], J. Alexandra Rowe[1]

[1]Institute of Immunology and Infection Research, School of Biological Sciences, University of Edinburgh, Edinburgh, United Kingdom. [2]KEMRI-Wellcome Laboratories, Kilifi, Kenya. [3]Institute of Infection, Immunity and Inflammation, University of Glasgow, Glasgow, United Kingdom.

Short title: identification of novel PfEMP1 variants that mediate rosetting

*joint first authors

Abstract

Plasmodium falciparum erythrocyte membrane protein 1 (PfEMP1) is a diverse family of variant surface antigens, encoded by *var* genes, that mediates binding of infected erythrocytes to human cells and plays a key role in parasite immune evasion and malaria pathology. The increased availability of parasite genome sequence data has revolutionised the ability to study PfEMP1 diversity across multiple *P. falciparum* isolates. However, making functional sense of genomic data relies on the ability to infer binding phenotype from *var* gene sequence. For *P. falciparum* rosetting, the binding of infected erythrocytes to uninfected erythrocytes, the analysis of *var* gene/PfEMP1 sequences encoding the phenotype is limited, with only eight rosette-mediating PfEMP1 variants described to date. These known rosetting PfEMP1 variants fall into two types, characterised by N-terminal domains known as "domain cassette" 11 (DC11) and DC16. Here we test the hypothesis that DC11 and DC16 are the only PfEMP1 types in the *P. falciparum* genome that mediate rosetting, by examining a set of thirteen recent culture-adapted Kenyan parasite lines. We first analysed the *var* gene/PfEMP1 repertoires of the Kenyan lines and identified an average of three DC11 or DC16 PfEMP1 variants per genotype. *In vitro* rosette selection of the parasite lines yielded four with a high rosette frequency, and analyses of their *var* gene transcription, infected erythrocyte PfEMP1 surface expression, rosette disruption and erythrocyte binding function identified four novel rosette-mediating PfEMP1 variants. Two of these were of the predicted DC11 type (one showing the dual rosetting/IgM-Fc-binding phenotype), whereas two contained DC15 (DBLα1.2-CIDRα1.5b) a PfEMP1 type not previously associated with rosetting. We also showed that a Thai parasite line expressing a DC8-like PfEMP1 binds to erythrocytes to form rosettes. Hence, these data expand current knowledge of rosetting mechanisms and emphasize that the PfEMP1 types mediating rosetting are more diverse than previously recognised.

Author summary

Malaria is an infectious tropical disease caused by the parasite *Plasmodium falciparum* that kills more than half a million people every year, mostly young children in sub-Saharan Africa. Life-threatening episodes of malaria are characterised by huge numbers of parasitised red blood cells in the infected host, many of which bind to blood vessel walls and block blood flow, causing tissue damage and organ failure. Sometimes parasitised red cells also bind to uninfected red cells to form clusters of cells called rosettes, which make the blockage of blood flow in vital organs even worse. Previous research has begun to decipher how parasitised red cells bind to uninfected red cells to form rosettes, but little is yet known about the process. Here we identify some new versions of the "sticky proteins" (adhesion molecules) that are made by malaria parasites and displayed on the surface of infected red cells to bring about rosette formation. The rosette-mediating adhesion molecules are members of a large family, and we identify here a few characteristic types within this family that mediate rosetting. This work is an important step towards the goal of understanding how malaria parasite rosettes form rosettes in order to develop preventions or treatments to reverse rosetting and reduce the number of people dying from severe malaria.

56 **Introduction**

57 Rosetting is the binding of erythrocytes parasitised with *Plasmodium spp.* to uninfected erythrocytes
58 during the asexual blood stage of malaria infection, and has been described for *P. falciparum*, *P.*
59 *vivax*, *P. ovale* and *P. malariae*, as well as in murine and primate malaria parasite species (reviewed
60 by (1)). Rosetting is a phenotypically variable property, with different parasite isolates having
61 between zero and >90% of mature-infected erythrocytes in rosettes (2). The rosetting phenotype is
62 of particular interest in *P. falciparum* malaria, because studies in Sub-Saharan Africa have
63 consistently shown that parasite isolates from severe malaria cases have significantly higher levels of
64 rosetting than those from uncomplicated malaria cases (2-5), raising the possibility that rosetting
65 contributes to disease pathogenesis. Subsequent work has shown that rosettes are stable under
66 physiological blood flow shear forces and enhance microvascular obstruction caused by the
67 sequestration of infected erythrocytes (6-9). Furthermore, human erythrocyte polymorphisms that
68 reduce the ability of *P. falciparum* to form rosettes, such as blood group O and the Complement
69 Receptor One (CR1)-related Knops blood group, have been selected to a high frequency in malaria
70 endemic regions and are associated with significant protection against severe disease (10-12),
71 supporting the hypothesis that rosetting is a parasite virulence-associated phenotype.

72 Rosetting in *P. falciparum* infected erythrocytes begins at ~16-20 hours post invasion, a
73 time-point corresponding to the appearance of parasite-derived variant antigens on the infected
74 erythrocyte surface (13). Specific members of the variant surface antigen family *P. falciparum*
75 Erythrocyte Membrane Protein 1 (PfEMP1) are the best characterised rosette-mediating parasite
76 adhesion molecules in *P. falciparum* (14-17), although there is some limited evidence to suggest that
77 other VSA families such as the RIFINs and STEVORs may contribute to rosetting in some parasite
78 genotypes (18, 19). PfEMP1 is encoded by *var* genes that can be classified into three main groups A,
79 B and C and two intermediate groups B/A and B/C by their conserved upstream promoter sequences
80 (20). These groups have functional significance as parasite isolates causing severe malaria
81 predominantly transcribe group A and B/A *var* genes (21-25). PfEMP1 variants have an N-terminal

82 'head structure' composed of an N-terminal sequence (NTS) and Duffy Binding Like (DBL) domain
83 followed by a Cysteine-rich InterDomain Region (CIDR)(26). Downstream from the head structure, a
84 variable number of further DBL and CIDR domains comprise the rest of the extracellular region.
85 PfEMP1 DBL and CIDR domains have been classified using phylogenetic methods into seven (α, β, γ,
86 δ, ε, ζ and pam) and five (α, β, γ, δ and pam) main classes respectively (26), which can be further
87 divided into numerical subclasses (27). Group A *var* genes encode DBLα1 domains, followed by a
88 CIDRα1 or CIDRβ/γ/δ domain in their head structures, whereas group B and C *var* genes encode
89 DBLα0 domains followed by CIDRα2-6 domains (26, 27). Domain subclasses frequently found
90 together in tandem are called domain cassettes (DCs) (27).

91 PfEMP1 groups, domain cassettes and domain subclasses have been linked to specific host
92 receptor binding phenotypes (reviewed in (28)), and the PfEMP1 domains that bind to host
93 endothelial cell receptors such as CD36 (29), ICAM-1 (30) and endothelial cell protein receptor
94 (EPCR) (31) are well-characterised. However, current understanding of the molecular interactions
95 that cause rosetting is based on just eight PfEMP1 variants from six culture-adapted *P. falciparum*
96 genotypes (14, 15) (17, 32). Seven of the eight characterised rosette-mediating PfEMP1 variants are
97 encoded by group A *var* genes, and have a DBLα1 domain of subclass 1.5, 1.6 or 1.8 (Figure 1A).
98 These domains are followed by a CIDRβ, γ or δ domain, completing DC11 in two of the characterised
99 rosetting variants (IT4VAR60 and TM284VAR1), DC16 in three variants (3D7PF13_000, HB3VAR06
100 and MUZ12 VAR1) and DC16-like (similar to DC16, but with CIDRγ rather than CIDRδ) in two variants
101 (IT4VAR09 and PAVARO) (Figure 1B). These domain classes and cassettes therefore define a
102 rosetting-associated head structure (DBLα1.5/6/8-CIDRβ/γ/δ).

103 A single previously characterised candidate rosetting variant, TM180VAR1, is encoded by a
104 group B/A *var* gene that lacks the rosetting-associated head structure (17). This gene has a "DC8-
105 like" head structure, with a DBLα2 domain followed by a CIDRα1.8 domain (Figure 1A), whereas DC8
106 usually has a CIDRα1.1 domain (Figure 1B) (27). The unusual architecture of this variant, along with
107 the observation that antibodies against the DBLα domain did not disrupt rosettes in this parasite line

108 (17), means that the evidence supporting this as a rosette-mediating PfEMP1 type is weaker than for
109 the other reported variants, and it remains possible that the TM180 parasite line forms rosettes via a
110 PfEMP1-independent mechanism.

111 Due to the small number of characterised rosetting PfEMP1 variants to date, we currently
112 lack a model to predict with confidence from parasite genomic sequence data which PfEMP1
113 variants mediate rosetting and which do not. In this study, we hypothesized that the rosetting
114 phenotype in diverse *P. falciparum* isolates is encoded by either DC11 or DC16 PfEMP1 variants. We
115 tested this hypothesis by firstly identifying PfEMP1 variants with the predicted rosetting head
116 structure in the genomes of thirteen recently culture-adapted Kenyan *P. falciparum* lines, then
117 selected four of these lines for rosetting and characterised their *var* gene/PfEMP1 expression. We
118 also examined whether the DC8-like candidate rosetting variant TM180VAR1 has erythrocyte-
119 binding function. Our findings confirm the importance of DC11 and DC8-like variants in rosetting
120 and identify another previously unrecognised PfEMP1 domain cassette (DC15) that binds to
121 uninfected erythrocytes to mediate rosette formation.

122

123 **Results**

124 ***Selection of high rosetting (R+) Kenyan P. falciparum lines***

125 Thirteen culture-adapted *P. falciparum* lines, originally isolated from children with *P. falciparum*
126 malaria in Kenya, were studied (33, 34). The full *var* gene/PfEMP1 repertoire sequences of these
127 parasites were published previously (35), and are shown in diagrammatic form in Figure S1. On
128 examining the repertoires, the number of PfEMP1 variants with the predicted rosetting-associated
129 head structure (DBLα1.5/6/8-CIDR$\beta/\gamma/\delta$) ranged from 0 to 7 (median 3) per parasite line (Table 1).
130 We cultured each of the Kenyan *P. falciparum* lines for at least two replication cycles *in vitro* and
131 screened the mature-infected erythrocytes for spontaneous rosette formation by microscopy.
132 Rosettes were detected in four of the parasite lines, at a high level in KE10 (>50% of infected
133 erythrocytes in rosettes) and a low level in PC0053, KE11 and KE08 (2-10% of infected erythrocytes

134 in rosettes). The absence of rosetting in the other parasite lines, despite their genomes containing
135 group A *var* genes encoding PfEMP1 variants with the rosetting head structure, is not surprising
136 because previous work has shown that parasites tend to switch off group A *var* genes when adapted
137 to culture (36). The four rosette-positive lines were grown in continuous culture and selected using
138 density gradient methods to generate isogenic pairs of high rosetting (R+, >60% of infected
139 erythrocytes in rosettes) and low rosetting (R-, <2% of infected erythrocytes in rosettes) parasite
140 lines for each genotype. Parasite line KE11R+ was resistant to selection for a high rosette frequency
141 using conventional methods, possibly due to a high frequency of *var* gene switching. Therefore,
142 further study of KE11R+ was carried at a rosette frequency of ~15-30% of infected erythrocytes in
143 rosettes.

144

145 **Table 1.** The Kenyan *P. falciparum* parasite lines screened for the formation of rosettes *in vitro*.

Parasite line[#]	Pf3K designation[#]	Clinical syndrome*	Group A *var* genes[$]	Predicted rosetting head structure[†]	Rosettes seen *in vitro*	Human IgM-Fc binding[&]
9106	PFKE01	IC	7	1	No	ND
9626	PFKE02	UM	15	3	No	ND
8383	PFKE03	UM	9	2	No	ND
10668	PFKE04	IC, RD	14	4	No	ND
11014	PFKE05	SMA	6	2	No	ND
10936	PFKE06	UM	11	6	No	ND
10975	PFKE07	SMA	23	7	No	ND
9605	**PFKE08**	**IC**	**8**	**4**	**Yes**	**No**
6816	PFKE09	IC	6	0	No	ND
11019	**PFKE10**	**IC**	**10**	**3**	**Yes**	**Yes**
9775	**PFKE11**	**UM**	**13**	**3**	**Yes**	**No**
9215	PFKE12	RD	12	3	No	ND
9197	**PC0053**	**IC**	**8**	**3**	**Yes**	**No**

146 [#]The name of each parasite line according to the KEMRI-Wellcome Trust Laboratory parasite naming
147 system (33, 34) and its designation in the Pf3k database (35) is given.
148 *The clinical syndrome of the patient from whom the parasite isolate was collected. IC, impaired
149 consciousness; UM, uncomplicated malaria: RD, respiratory distress; SMA, severe malarial anaemia.
150 [$]The total number of group A *var* genes in each parasite's genome.
151 [†]The number of *var* genes in each parasite's genome that encode the rosetting-associated head
152 structure DBLα1-CIDRβ/γ/δ.
153 [&]Determined by immunofluorescence assay/flow cytometry of live infected erythrocytes with an
154 anti-human IgM (μ chain) antibody. ND, not done.
155
156
157 ***IgM-binding and trypsin-sensitivity of rosetting in the Kenyan R+ parasite lines***

158 Previous work has shown that some *P. falciparum* rosetting lines bind the Fc region of human IgM,
159 and this promotes rosette formation, possibly by clustering PfEMP1 molecules to increase binding
160 avidity (37-39). The dual rosetting and IgM-Fc binding phenotype is strongly associated with severe
161 malaria (40, 41) and the known PfEMP1 variants that mediate this dual binding are mostly of the
162 DC11 type (Figure 1) (17, 37, 38, 42). Due to the presence of human serum in the parasite culture
163 medium, IgM-binding can be detected by immunostaining of live infected erythrocytes taken directly
164 from culture. Hence, the four R+ lines were assessed for their IgM-binding ability by staining with
165 anti-human IgM antibodies. Infected erythrocytes of the KE10R+ parasite line were IgM positive,
166 whereas the other three R+ lines were IgM negative (Figure 2A, Table 1).

167 PfEMP1 is characteristically highly sensitive to trypsin digestion (17, 43), whereas RIFINs and
168 STEVORS, which have also been implicated in rosetting, are not (44, 45). Therefore, to determine
169 whether PfEMP1 was the likely rosette-mediating parasite adhesion molecule in the Kenyan
170 rosetting lines, infected erythrocytes were treated with a low dose of trypsin and rosette frequency
171 was assessed. Rosetting in all four lines was abolished by treatment with 1μg/ml trypsin for five
172 minutes, consistent with a PfEMP1-dependent rosetting mechanism (Figure 2B).

173

174 ***var gene profiling to identify predominant rosetting-associated PfEMP1 variants***

175 To identify the predominant *var* genes specifically transcribed in the R+ parasite lines, we carried out
176 DBLα tag profiling of the R+/R- isogenic pairs (14, 46). The full *var* gene sequence for each

177 predominant tag was retrieved from the Pf3k database (35) or determined by extension PCR and
178 sequencing. For clarity, the predominant rosette-specific *var* gene identified in each parasite line is
179 referred to here as *'parasite line name var_r1'* with the full name of each gene from the Pf3K
180 database also given on first use. *var* gene profiling of KE10R+ and KE10R- parasite lines showed that
181 the *pfke10var_r1* (*PX0203.g54)* gene encoding a DC11 PfEMP1 variant was the predominant
182 transcript expressed only in the rosetting line (Figure 3 and Figure 4). Parasite lines PC0053R+ and
183 KE11R+ both expressed two predominant transcripts. However, in each case, only one was
184 exclusively expressed by the R+ line (Figure 3). Therefore, *pc0053var_r1 (PC0053-C.g687)* and
185 *pfke11var_r1 (PFKE11.g448),* encoding PfEMP1 variants containing DC15 (DBLα1.2-CIDRα1.5b), were
186 identified as the candidate rosette-mediating adhesins (Figure 4). This head structure has not
187 previously been associated with rosetting. *var* gene profiling of the KE08R+ and KE08R- parasite lines
188 identified two predominant transcripts in the R+ population, *pfke08var_r1 (PFKE08.g502)* and
189 *pfke08var_r2 (PFKE08.g501)* (Figure 3). Expression of *pfke08var_r2* was not detected in the R-
190 population, whereas *pfke08var_r1* was detected at a low level (5% of transcripts). *pfke08var_r1*
191 encodes a DC11 rosetting-associated head structure, whereas *pfke08var_r2* is a group B/A *var* gene,
192 encoding DC8 (DBLα2-CIDRα1.1) (Figure 4). DC8 PfEMP1 variants are usually associated with binding
193 to human brain endothelial cells via EPCR (47), and not with rosetting, with the exception of the
194 unusual putative rosetting variant TM180VAR1, which has a "DC8-like" architecture (17). Therefore,
195 in this case, both *pfke08var_r1* and *pfke08var_r2* were considered to be potential rosette-mediating
196 PfEMP1 variants and were investigated further.
197
198 ***Staining of infected erythrocytes for surface expression of candidate rosetting-associated variants***
199 We next raised antibodies to the candidate rosetting PfEMP1 variants identified above, to determine
200 whether the specific PfEMP1 variants were present on the surface of live infected erythrocytes. The
201 NTS-DBLα region of each variant was expressed as a recombinant protein in *E. coli* (Figure S2) and
202 used to immunise rabbits to generate polyclonal antibodies against PfEMP1 as described previously

203 (17, 48). The antibodies were used in indirect immunofluorescence and flow cytometry with live
204 infected erythrocytes. Non-immunised rabbit IgG or IgG raised to an irrelevant PfEMP1 NTS-DBLα
205 protein (HB3VAR03, which binds to human brain endothelial cells (49)) were used as negative
206 controls, and the gating strategy to identify the mature pigmented-trophozoite and schizont stage
207 infected erythrocyte population which displays PfEMP1 as a DNA/RNA high population is shown in
208 Figure S3.

209 In each case, the IgG against the candidate rosetting PfEMP1 variant stained live rosetting
210 infected erythrocytes of the respective parasite line at a frequency comparable to the rosette
211 frequency, whereas the isogenic R- lines were negative (Figure 5). Unexpectedly, in the KE08R+ line
212 ~90% of mature infected erythrocytes stained positively with both the KE08VAR_R1-specific rabbit
213 IgG and the KE08VAR_R2-specific IgG (Figure 5E and G). This suggests either antibody cross-reactivity
214 or the possibility that both PfEMP1 variants are expressed on the same infected erythrocytes.
215 Usually only one PfEMP1 type is expressed per infected erythrocyte, due to mutually exclusive
216 expression of *var* genes (50). However, one previous example of a parasite line simultaneously
217 expressing two different PfEMP1 variants on the same infected erythrocyte has been described (51).
218 To examine KE08R+ in more detail, we raised antibodies against the N-terminal CIDR domains of the
219 two predominantly expressed PfEMP1 types and repeated the immunofluorescence staining. Once
220 again, the polyclonal rabbit IgG raised against the KE08VAR_R1 CIDR domain and the KE08VAR_R2
221 CIDR domain both stained a similar major population of infected erythrocytes in the rosetting line,
222 consistent with expression of both variants on the surface of infected erythrocytes (Figure 5I and K).
223

224 ***Rosette disrupting activity of anti-PfEMP1 IgG***

225 Next, we assessed the ability of the rabbit IgG raised against the candidate rosetting variants to
226 disrupt rosettes in their respective lines. IgG from antisera raised to the NTS-DBLα domain of an
227 irrelevant PfEMP1 variant (HB3VAR03) and IgG purified from the sera of a non-immunised rabbit
228 were used as negative controls. The KE11R+ line was not included in these assays, due to the

229 difficulty in maintaining a sufficiently high level of rosetting. For parasite lines KE10R+ and
230 PC0053R+, rosetting was completely abolished by 10μg/ml of rabbit IgG to the relevant PfEMP1 NTS-
231 DBLα domain (Figure 6A and B), supporting the identification of KE10VAR_R1 (DC11) and
232 PC0053VAR_R1 (DC15) as rosette-mediating PfEMP1 types. In the KE08R+ line, rosettes were
233 abolished by 10μg/ml of IgG to the NTS-DBLα domain of KE08VAR_R1 (DC11), but there was no
234 effect on rosetting of IgG to KE08VAR_R2 (DC8) (Figure 6C), despite these antibodies recognising the
235 surface of KE08R+ infected erythrocytes (Figure 5G). This suggests that it is the DC11 variant
236 KE08VAR_R1 and not the DC8 variant KE08VAR_R2 that is the rosette-mediating adhesion molecule
237 in the KE08R+ parasite line.
238
239 ***Functional assays to detect PfEMP1 binding to uninfected erythrocytes and IgM***
240 Previous studies have identified the NTS-DBLα domain as the erythrocyte-binding region of rosette-
241 mediating PfEMP1 variants (14, 15, 17, 32). To examine the erythrocyte binding function of the
242 candidate rosetting variants, NTS-DBLα and CIDR recombinant proteins were incubated with
243 uninfected erythrocytes and bound protein detected by flow cytometry. The NTS-DBLα domain of
244 the well-characterised rosetting variant IT4var60 (15, 17) was included as a positive control,
245 alongside negative controls which were NTS-DBLα domains from human brain endothelial cell
246 binding PfEMP1 variants that are expressed by parasite lines that are known to be non-rosetting
247 (49).
248 The NTS-DBLα domains of the candidate rosetting variants KE10VAR_R1 (DC11),
249 PC0053VAR_R1 (DC15), KE11VAR_R1 (DC15) and KE08VAR_R1 (DC11) all bound to uninfected
250 erythrocytes, confirming their identification as rosette-mediating variants (Figure 7A-F). Neither the
251 NTS-DBLα or CIDR domain from KE08VAR_R2 bound to erythrocytes, consistent with the above
252 suggestion that KE08VAR_R2 is not a rosette-mediating variant (Figure 7A and G). The CIDR domains
253 of KE08VAR_R1 and KE11VAR_R1 also did not bind to erythrocytes, consistent with previous data

254 showing NTS-DBLα to be the major erythrocyte-binding domain of rosette-mediating PfEMP1
255 variants (Figure 7A) (14, 32, 52).
256 For the IgM Fc-binding rosetting line KE10R+, the domains downstream of the head
257 structure were expressed as recombinant proteins and tested for human IgM binding by ELISA.
258 Previous work has identified either the ultimate DBLε or penultimate DBLζ domain as the IgM-
259 binding region of PfEMP1 (Figure 1) (37-39, 53). Consistent with this, DBLζ3 was identified as the
260 IgM-binding domain of KE10VAR_R1 (Figure 8).
261
262 ***The "DC8-like" variant TM180VAR1 mediates rosetting***
263 The rosetting line TM180R+ expresses the group B/A *var* gene *tm180var1*, which lacks the rosetting
264 associated head structure (Figure 1) (17). To test the hypothesis that TM180R+ forms rosettes via a
265 variant surface antigen other than PfEMP1, TM180R+ was treated with low-dose trypsin as
266 described above. TM180R+ rosetting was abolished by 5 μg/ml of trypsin, suggestive of a PfEMP1-
267 mediated rosetting mechanism rather than an alternative RIFIN- or STEVOR-mediated mechanism
268 (Figure 9A). The TM180VAR1 NTS-DBLα recombinant protein was tested in the erythrocyte binding
269 flow cytometry assay, and showed unequivocal binding to uninfected erythrocytes, confirming its
270 role in rosetting (Figure 9B).
271
272 ***KE08R+ binds to ICAM-1 and EPCR as well as forming rosettes***
273 The simultaneous expression and surface display of KE08VAR_R1 and KE08VAR_R2 shown above
274 raise the possibility that the KE08R+ parasite line might have an unusual adhesion phenotype.
275 KE08VAR_R2 contains CIDRα1.1 and DBLβ12 domains, that characteristically bind EPCR and ICAM-1,
276 respectively (30, 47). Static binding experiments showed that KE08R+ infected erythrocytes bound to
277 EPCR and ICAM-1 (Figure 10). Notably, significantly higher binding was seen when rosettes were
278 disrupted with rabbit IgG to KE08VAR_R1 prior to the binding assay, suggesting that once rosettes
279 have formed, they impede binding to other receptors in adhesion assays, as shown previously (54).

280 This suggests that, by expressing two *var* genes simultaneously, KE08R+ infected erythrocytes exhibit
281 an unusual "triple" virulence-associated adhesion phenotype - rosetting, ICAM-1 binding and EPCR-
282 binding.
283
284 ***Presence of rosetting-associated motifs and binding sites in the novel rosetting PfEMP1 variants***
285 Having identified four new rosette-mediating PfEMP1 variants, we examined a multiple sequence
286 alignment of known rosetting and non-rosetting NTS-DBLα amino acid sequences to determine if
287 previous motifs (4) and homology blocks (HB) (55) associated with high rosetting are found in the
288 new variants and are conserved across all rosetting variants. The motif "MFKPNKDKVEG" that
289 contains HB219 (55) and the adjacent high rosetting "H3" motif (4) was seen in all of the newly
290 described variants and this sequence is over-represented in rosetting compared to non-rosetting
291 variants (green box, Figure 11). The other Normak et al (4) high rosetting motifs (H1 and H2) were
292 not found. Two other motifs in the central region of NTS-DBLα "YKDGSG" (red box, Figure 11) and
293 "TCKAPQDAN" (blue box, Figure 11) were found in the newly identified variants and are strongly
294 over-represented in the rosetting variants overall.
295
296 **Discussion**
297 Here we have identified four novel rosette-mediating PfEMP1 variants, determined by *var* gene
298 profiling, infected erythrocyte surface expression of PfEMP1, rosette disruption with antibodies to
299 PfEMP1 and functional studies showing NTS-DBLα binding to uninfected erythrocytes. Two of the
300 variants identified, KE10VAR_R1 and KE08VAR_R1 contain DC11, giving them comparable PfEMP1
301 architecture to the previously described rosetting variants TM284VAR1 and IT4VAR60 (Figure 1) (15,
302 17, 37). The other two new rosetting variants, PC0053VAR_R1 and KE11VAR_R1, have a DC15 head
303 structure, not previously implicated in rosetting. Instead, DC15 PfEMP1 variants were thought to
304 bind EPCR via their CIDRα1.5 domain (31). However, CIDRα1.5 domains fall into two clear subtypes,
305 CIDRα1.5a and CIDRα1.5b (31). The DC15 variants identified here have an NTS-DBLα1.2 domain that

306 binds to erythrocytes (Figure 7), followed by CIDRα1.5b, a domain type which when investigated
307 previously only bound weakly to EPCR (31). Thus, rosetting DC15 variants may represent a
308 functionally distinct group, possibly characterised by the presence of CIDRα1.5b (Figure S4),
309 although further work is needed confirm this. Our study also showed that the NTS-DBLα2 domain of
310 a "DC8-like" variant encoded by *tm180var1* binds to uninfected erythrocytes, confirming this as a
311 rosette-mediating variant (17).

312 These findings combined with previous work show that at least four different group A and
313 B/A PfEMP1 types mediate rosetting: DC11, DC16, DC15 (with CIDRα1.5b) and DC8-like, with only
314 the first two containing the recognised rosetting-associated head structure of DBLα1.5/6/8-
315 CIDRβ/γ/δ. It remains unknown whether these different rosette-mediating PfEMP1 types have
316 functional significance, for example, binding to different host receptors on uninfected erythrocytes
317 (56), and this should be explored in future. Recent work also suggests that a group C PfEMP1 variant
318 PF3D7_0412900 can mediate rosetting by binding to Glycophorin B on uninfected erythrocytes (57).
319 Taken together, these data show that a more diverse set of PfEMP1 types mediates rosetting than
320 originally recognised. Further investigation will be needed to determine whether all PfEMP1 variants
321 containing these particular rosetting-associated DCs mediate rosetting. Our analysis of the *var* gene
322 repertoires of the thirteen Kenyan parasite lines showed that on average, there are three *var* genes
323 per *P. falciparum* genome encoding a DC11 and/or DC16 variant (Table 1). Many of these parasite
324 lines also have one or more *var* gene encoding a DC15 (CIDRα1.5b) and/or a DC8-like variant
325 containing a CIDRα1.8 domain rather than the CIDRα1.1 found in classical non-rosetting EPCR-
326 binding DC8 variants (31). If the DC types identified here always mediate rosetting, this would imply
327 that about one third of the group A and B/A *var* genes per *P. falciparum* isolate encode rosetting
328 variants, consistent with an important biological role for this phenotype. Exactly how rosetting
329 benefits the parasite is unclear, but an *in vivo* model showed that rosetting parasites reach a high
330 parasite burden more rapidly than isogenic non-rosetting parasite (58), which could increase
331 parasite fitness by enhancing transmission (59). More rapid expansion *in vivo* could be due to

332 rosetting enhancing erythrocyte invasion or reducing immune-mediated clearance, with current
333 experimental evidence favouring the latter hypothesis (60-62).

334 Previous work has demonstrated a strong association between rosetting and severe malaria
335 (2-5), with human IgM-binding rosetting isolates being particularly common in parasites collected
336 from African children with severe malaria (40, 41). Whether all rosetting phenotypes mediated by
337 the different DC types shown here have associations with severe malaria is unknown. Analyses of
338 parasite *var* gene transcription and clinical malaria severity have repeatedly shown that expression
339 of group A *var* genes and those encoding DC8 are associated with severe disease (21-25). As shown
340 here and previously (17, 37), the IgM-binding rosetting phenotype is mediated by DC11 or DC16
341 PfEMP1 variants, and a recent study found expression of DC11 was associated with severe malaria in
342 Mozambiquan children (63), while both DC16 and DC15 were associated with severe malaria in
343 malaria-naïve adults (64). Many prior studies on *var* gene transcription and malaria severity do not
344 include primer sets for DC11 (22, 24, 25), raising the possibility that the contribution of this IgM-
345 binding rosette-mediating variant type to severe malaria could be greater than currently
346 appreciated. Understanding how *var* gene transcription relates to parasite adhesion phenotype is
347 important in facilitating the interpretation of *var* gene profiling/disease severity studies and can help
348 identify the key adhesion phenotypes that should be targeted therapeutically to treat or prevent
349 severe disease.

350 One of the most underexplored topics in rosetting research is understanding how rosettes
351 sequester *in vivo*. Rosettes do not circulate in the peripheral blood and "rosette-like" aggregates of
352 infected and uninfected cells can be seen in the microvasculature in autopsy studies of cerebral
353 malaria patients (65-67). Sequestration of rosetting infected erythrocytes may require a dual
354 binding phenotype with simultaneous binding to receptor(s) on vascular endothelium as well as on
355 erythrocytes (68, 69). However, host endothelial cell receptors for rosetting PfEMP1 variants remain
356 poorly characterised. One in vitro study found that the rosetting line IT4VAR09/R29R+, which
357 expresses a DC16-like variant (Figure 1), adhered to a human brain endothelial cell line via the

358 DBLγ15 domain, which interacted with an unidentified host heparan sulfate proteoglycan (69). It is
359 notable that all of the experimentally-proven rosetting variants, including the four new ones
360 described here, contain DBLγ as the third or fourth extracellular domain from the N-terminus, and
361 we hypothesize that binding of DBLγ to endothelial cell heparan sulfate is a common mode of
362 sequestration for rosetting infected erythrocytes. It is plausible that the diverse CIDRβ/γ/δ/α1
363 domains of rosetting variants may alos bind to additional host receptors, and this remains to be
364 explored.

365 Another feature of some rosette-mediating variants is the ability to bind serum proteins
366 such the human IgM-Fc and α2M, a phenomenon that clusters PfEMP1 to increase binding avidity
367 (37, 38) (39, 42). The IgM-Fc binding rosetting variants identified to date all contain a C-terminal
368 triplet of DBLε and DBLζ domains (17), but only one of these domains in each variant binds IgM (37-
369 39, 53). We show here that KE10R+ infected erythrocytes bind IgM via the DBLζ3 domain of
370 KE10VAR_R1, consistent with previous data. Interestingly, the KE08R+ and PC0053R+ parasite lines
371 did not bind IgM, despite their PfEMP1 variants containing a C-terminal DBLε/ζ domain triplet
372 (Figure 4). Therefore, the presence of a C-terminal DBLε/ζ domain triplet is not always predictive of
373 IgM binding in rosetting variants, although in the case of KE08R+, the expression of two different
374 PfEMP1 variants at the surface of infected erythrocytes might interfere with binding function at the
375 membrane-proximal part of PfEMP1.

376 The majority of evidence to date suggests that expression of PfEMP1 is mono-allelic (50, 70).
377 However, here we clearly demonstrate the simultaneous expression of two different group A
378 PfEMP1 variants on the surface of infected erythrocytes of parasite line KE08R+, one mediating
379 rosetting and the other binding to EPCR and ICAM-1. A similar finding was reported previously, with
380 a *P. falciparum* 3D7 parasite line expressing two PfEMP1 variants PFD1235w and PF11_0008,
381 conferring a dual binding phenotype to PECAM-1 and ICAM-1, which increased binding efficiency to
382 endothelial cells (51). Dual binding phenotypes are more commonly described in the context of
383 single PfEMP1 variants, with different domains within the same molecule binding different receptors

384 (30, 69). It seems likely that the ability to adhere to multiple receptors is advantageous to the
385 parasite by strengthening adhesion and thereby promoting sequestration. The multiple adhesion
386 phenotypes seen in both KE08R+ and the 3D7 line described above could be artefactual, for example
387 with loss of mono-allelic *var* gene transcription due to mutations introduced by the culture
388 adaptation process. Or they could represent genuine aspects of parasite biology that remain to be
389 explored. Existing bulk RNA *var* gene profiling studies in clinical isolates would not detect polygenic
390 *var* gene transcription, and single cell studies of clinical isolates will be needed to determine
391 whether multiple *var* genes are transcribed per infected erythrocyte in natural infections.

392 The increasing availability of *var* gene sequence data has revolutionised the ability to study
393 PfEMP1 diversity across multiple *P. falciparum* isolates (35). However, making functional sense of
394 these data relies on the ability to infer binding phenotype from *var* gene sequence. Excellent
395 progress has been made with PfEMP1 variants that bind to CD36, ICAM-1 and EPCR (29-31), and the
396 work described here is a step towards a more comprehensive understanding of rosette-mediating
397 PfEMP1 variants. Important unanswered questions for future work include how many different
398 PfEMP1 types mediate rosetting, which host receptor(s) are they binding and are they suitable
399 targets for interventions such as strain-transcending antibodies to treat or prevent severe malaria
400 (17, 71)?

401

402 **Materials and Methods**

403 ***Ethics statement***

404 Human erythrocytes and serum were obtained after informed written consent from donors at the
405 Scottish National Blood Transfusion Service (SNBTS), Edinburgh, UK. Ethical approval was granted
406 from the University of Edinburgh, School of Biological Sciences Ethical Review Panel (arowe002) and
407 the Scottish National Blood Transfusion Service (SNBTS) Ethics Review Board (19~6 and 22~11).

408 ***Parasite culture and rosette selection***

409 The Kenyan parasite lines (Table 1) were originally derived from children with severe or
410 uncomplicated *P. falciparum* malaria between 2009 and 2010 in Kilifi, Kenya and were adapted to
411 culture previously (33) at the Wellcome-Kenya Medical Research Institute (KEMRI) laboratories. The
412 parasite lines are available from the European Malaria Reagent Repository
413 (http://www.malariaresearch.eu/). Parasites were thawed and cultured in complete RPMI with 5%
414 pooled human serum and 0.25% albumax and human blood group O erythrocytes as described (71).
415 Isogenic pairs of high and low rosetting cultures were selected using density gradient methods (72).

416 ***Analysis of the var gene repertoires of the Kenyan parasite lines***

417 The PfEMP1 domain boundaries and architecture for the Kenyan parasite lines were obtained from a
418 previous study (35). The PfEMP1 repertoire for each parasite line was plotted using R v4.2.2 (73) and
419 arranged based on the 5' ups group of each protein (A, B then C). The domains were colour-coded as
420 previously described (27). The PFKE10VAR1 domain architecture was generated as described in the
421 *pfke10var1* sequence extension section below.

422 ***Assessment of rosette frequency***

423 Rosette frequency was assessed by staining an aliquot of culture suspension at ~2% haematocrit
424 with ethidium bromide (final concentration 25 μg/ml) and examination of a wet preparation using
425 simultaneous fluorescence/bright field microscopy on a Leica DM 2000 fluorescent microscope with
426 a x40 objective. A rosette was defined as an infected erythrocyte binding at least two uninfected
427 erythrocytes, and the rosette frequency expressed as the proportion of infected erythrocytes
428 forming rosettes out of 200 infected erythrocytes counted.

429 ***IgM-binding - immunofluorescence and flow cytometry***

430 Staining for human IgM was performed by incubating aliquots of live parasite culture in PBS/1%BSA
431 with 20μg/ml rabbit IgG against PfEMP1 NTS-DBLα for 45 mins then washing three times with PBS.
432 The washed cells were incubated in PBS/1% BSA containing 1/2500 of Vybrant™ DyeCycle™ stain
433 with 1/1000 Alexa Fluor™ 647-conjugated cross-absorbed goat anti-rabbit IgG (Invitrogen, A-21244)
434 and 1/1000 Alexa Fluor™ 488-conjugated cross-adsorbed goat anti-human IgM (heavy chain

435 specific) (Invitrogen, A-21215) before washing as above and fixing in PBS/0.5% paraformaldehyde.
436 The samples were used to make thin smears for microscopy or read on a BD LSRFortessa instrument
437 (BD Biosciences) with data from least 500 mature parasitised erythrocytes collected per sample.
438 Data were analysed in FlowJo v.10 and the gating strategy is shown in Figure 2A. As a negative
439 control, parasites were grown as described above in complete RPMI but with 5% IgM-deficient
440 human serum, prepared by five consecutive 30 minute rounds of incubation with anti-human IgM
441 beads (Sigma-Aldrich A9935).

442 ***Trypsinisation of parasitised erythrocytes***

443 Mature pigmented trophozoites were purified from 100µl packed cell volume of parasite culture at
444 >4% parasitaemia using magnetic purification as described (71). The purified parasites were washed
445 twice before being resuspended in 100µl of trypsin (Sigma-Aldrich T4799) in PBS at concentrations 0,
446 0.5, 1 and 5µg/ml, and incubated at 37°C for 5 mins. Cells were pelleted by centrifugation and the
447 pellet resuspended in 1 mg/ml soybean trypsin inhibitor (Sigma-Aldrich T9003) and incubated at
448 37°C for 5 mins. The cell pellet was washed and resuspended in complete binding media (RPMI 1640
449 without bicarbonate with 25 mM HEPES, 16mM glucose, 25µg/ml gentamicin, and 10% human
450 serum). O+ blood was added to each sample to a final parasitaemia of 20%, mixed, and incubated at
451 37°C for 1 hour. The cells were then pelleted before being resuspended by gentle pipetting and
452 rosette frequency assessed. Samples were assayed in duplicate and the mean of the two rosette
453 frequency counts taken.

454 ***DBLα sequence tag RT-PCR***

455 RNA was extracted from parasite cultures when they at the mid-late ring/very early trophozoite
456 stage (~10-20 hours post invasion) by resuspending pelleted cells in 10x volumes of Trizol (Ambion
457 15596026). RNA was extracted, cleaned and concentrated using bromochloropropane (Sigma-
458 Aldrich B9673) and a Zymo Research RNA Clean & Concentrator Kit (R1014) according to the
459 manufacturer's instructions for Trizol clean-up with minor modifications. Samples were treated with
460 the TURBO DNase-Free Kit (Invitrogen AM1907) before cDNA was made from 8µl RNA using the

461 SuperScript ® III First-Strand Synthesis System for RT-PCR (Invitrogen 18080-051) with random
462 hexamers. DBLα-tag 50 µl PCR reactions contained 2µl of cDNA, 20.75 µl of dH_2O, 4 µl of 25mM
463 $MgCl_2$, 8 µl of 1.25mM dNTPs (Promega U120A, U121A, U122A, U123A), 5 µl of αAF2 primer
464 (GCACG(A/ C)AGTTT(C*/T)GC) (46), 5 µl of αBR primer (GCCCATTC(G/C)TCGAACCA) (46), and 5 µl of
465 Amplitaq Gold buffer with 0.25 µl Amplitaq Gold (1.25 units) (Applied Biosystems 4311816). The
466 reactions were cycled as follows, 95°C for 5 mins, 95°C for 20 s, 42°C for 20 s, 60°C for 1
467 minute, 60°C for 10 mins, 4°C to hold. The PCR products were cleaned using a Nucleospin
468 Gel and PCR Clean-up kit (Macherey-Nagel 740609.250) then cloned into the pCRII vector using a
469 TA Cloning Kit Dual Promoter pCRII Vector (Invitrogen K207020) at a vector to insert ration of 1:3.
470 TOP10F' One Shot Competent Cells (Invitrogen 440300) were transformed using 2µl of each ligation
471 reaction. 24 colonies were picked per ligation and grown overnight before plasmids were isolated
472 from the cultures using a GeneJET Plasmid Miniprep Kit (ThermoFisher Scientific K0502). Plasmid
473 inserts were Sanger sequenced at the MRC Protein Phosphorylation and Ubiquitiylation Unit,
474 Dundee (https://dnaseq.co.uk/) using the forward primer VF1 (AGCTCGGATCCACTAGTA) and the
475 resulting amino-acid sequences were used in a BLAST search (74) against the *var* gene/PfEMP1
476 repertoire of the relevant *P. falciparum* line to identify the full-length gene sequence.

477 **pfke10var1 sequence extension**

478 For completion of the *pfke10var1* Exon 1 sequence (which was incomplete in the database), a
479 forward primer (11019F2 5' GATTTTGACACATC CAAAGTGT) was designed targeting the *pfke10var1*
480 DBLZ3 domain at approximately 200bp from the end of the partial sequence. This was paired with a
481 reverse primer (Exon2_3.3 5' CCATTTCTTCATATTCACTTTC) targeting a conserved region in Exon 2
482 (75). 50pmols of each primer was added to a reaction mix containing 1.25mM dNTPs, 1.5mM $MgCl_2$,
483 1x Platinum *Pfx* buffer (Invitrogen 11708), 1 unit of Platinum *Pfx* DNA polymerase (Invitrogen
484 11708), 0.2µg cDNA and made up to a final reaction volume of 50µl. The PCR conditions were initial
485 denaturation at 95°C for 5 mins followed by 35 cycles of denaturation at 95°C for 5 secs, annealing at
486 52°C for 15 secs and extension at 60°C for 3 mins. A final extension was performed at 60°C for 10

487 minutes and the amplicon was resolved in a 1% agarose gel at 70V for 50 minutes to reveal a 2kb
488 band. This was then gel purified using a purification kit (Macherey-Nagel 740609) following the
489 manufacturer's instructions. The purified PCR product was Sanger sequenced using both the forward
490 and reverse sequences listed above. From the newly generated sequence from the forward primer,
491 another primer sequence was designed (11019P1 5' GAGTGTAAAGTTGAGTCCCTTG) targeting a
492 region approximately 400bp downstream which was then used to further sequence the original 2kb
493 PCR product. The Sanger sequencing results from the three primers (11019F2, 11019P1 and Exon 2)
494 and the partial Exon 1 sequence were then aligned to generate the complete Exon 1 sequence. To
495 define the domain boundaries of the complete KE10VAR_R1 Exon 1 protein sequence, the sequence
496 was submitted to VarDom (https://services.healthtech.dtu.dk/services/VarDom-1.0/)(27) for
497 annotation. The subclasses were resolved by using the individual domains in a BLAST search (74)
498 against the Pf3k database (35) and identifying the subclass of the top hit based on full length
499 alignment.

500 ***Recombinant protein production***

501 Codon optimised sequences for *E. coli* expression of PfEMP1 domains with a BamHI site at the 5' end
502 and an NheI site at the 3' end were obtained from Twist Biosciences (San Francisco, California) and
503 ligated into the expression vector modified pET15b (pET15b conv) (76). The DBLα domain sequences
504 included the N-terminal sequence. All proteins were synthesised with a His-tag at the N-terminal
505 end of the sequence. Ligation reactions were sequenced to confirm the correct insert sequence.
506 Origami B cells containing pRIG were transformed using the recombinant plasmids (76). Protein
507 expression was induced by the addition of IPTG and the bacteria harvested. Cell pellets were frozen
508 before resuspension in Bugbuster mastermix (Novagen 71456) and EDTA-free protease inhibitor
509 tablets (Roche 11836170001). Nickle-NTA or cobalt-NTA chromatography was used to purify the
510 polyhistidine (His)-tagged proteins. DBLα proteins were further purified by size exclusion
511 chromatography as described (17). For proteins KE10VAR_R1 DBLα, TM180VAR1 DBLα and
512 PC0053VAR_R1DBLα the his-tag was cleaved with TEV protease before use in experiments as

513 described (17, 48). Fractions containing protein were pooled and buffer exchanged into PBS using
514 PD-10 desalting columns (Sigma-Aldrich GE17-0851-01). The proteins were concentrated using
515 Vivaspin 20ml 10 kDa or 30 KDa MWCO concentrators (Merck Z614602-12EA) and stored in aliquots
516 at -70 °C.

517 ***Rabbit immunisations and IgG purification from antisera***

518 Rabbit immunisations were done by BioGenes GmBH (Berlin, Germany). Preimmune sera were
519 screened to identify rabbits that did not have anti-human erythrocyte antibodies by
520 immunofluorescence assay as described (17, 48). Selected rabbits were immunised with 250µg of
521 antigen in BioGenes proprietary adjuvant (92.8% mineral oil, 3.48% Tween-20, 3.48% Span-80 and
522 0.23% lipopolysaccharides from *Phormidium spp*) on day 1 followed by boosting with 100µg of
523 antigen on days 7, 14, 28, 49 with the final bleed on day 56. Total IgG was purified from the resulting
524 antisera using a Pierce protein A IgG purification kit (ThermoFisher Scientific 44667) according to the
525 manufacturer's instructions.

526 ***Flow cytometry with PfEMP1 antibodies***

527 Staining of mature parasitised erythrocytes for PfEMP1 with rabbit IgG was done as described (71).
528 Briefly, whole culture was incubated for 45 minutes with rabbit IgG against the relevant PfEMP1
529 domain at a final concentration of 20µg/ml before being washed three times with PBS. The cells
530 were then incubated in PBS/1% BSA containing 1/2500 of VybrantTM DyeCycle™ stain with 20µg/ml
531 ethidium bromide and 1/1000 Alexa Fluor 647-conjugated cross-adsorbed goat anti-rabbit IgG
532 (Invitrogen A-21244) for 30 minutes. Cells were washed twice in PBS and once in PBS 1% BSA before
533 being fixed in PBS/0.5% paraformaldehyde. The samples were read on a BD LSRFortessa instrument
534 (BD Biosciences) in duplicate with at data from least 500 mature parasitised erythrocytes collected
535 per sample. Data were analysed with FlowJo v.10.

536 ***Rosette disruption assays***

537 Parasite culture at ~2% haematocrit was stained with ethidium bromide at a final concentration of
538 25µg/ml for 2 mins at 37°C. The cells were pelleted by centrifugation, the supernatant removed, and

539 the pellet resuspend at 2% haematocrit in complete binding medium as described above. 2.5µl of
540 the relevant anti-PfEMP1 rabbit IgG at 100, 10 or 1µg/ml was added to 22.5µl aliquots of stained
541 culture to give final concentrations of 10, 1 and 0.1µg/ml. An equivalent volume of PBS was added to
542 the no antibody control. The samples were incubated at 37°C for 1 hour in the dark with gentle
543 resuspension of cells every 10 mins before assessment of rosette frequency. Statistical analyses and
544 graphs were done using GraphPad Prism (Version 10.2.2, GraphPad software, Inc).

545 ***Erythrocyte binding assays***

546 The assay investigating the ability of recombinant PfEMP1 domains to bind to uninfected
547 erythrocytes was based on those described previously (52, 77). 10 µl of washed O+ erythrocytes
548 were re-suspended in 1ml PBS/1% BSA with 100µg/ml of recombinant protein and incubated on ice
549 for 1 hour then washed twice with 200 µl ice-cold PBS and resuspended in 23.75 µl of PBS/1% BSA.
550 1.25 µl of the relevant rabbit IgG to the recombinant protein PfEMP1 domain at 1 mg/ml (final
551 concentration 50 µg/ml) was added and incubated on ice for 45 mins before washing twice with
552 500µl PBS. The washed cell pellets were resuspended in 50µl of PBS/1%BSA containing 1:1000
553 dilution of Alexa Fluor™ 488 goat anti-rabbit IgG (Invitrogen A-11034) and incubated for a further 45
554 mins on ice in the dark before being washed twice. The cells were resuspended in 200µl of PBS
555 containing 0.1% BSA and 0.01% sodium azide and transferred to a 96 well plate. The 96 well plates
556 were read on a BD LSRFortessa instrument (BD Biosciences). Data were analysed in FlowJo v.10. For
557 statistical analysis, median fluorescence intensity (MFI) values were log transformed and analysed by
558 one way ANOVA in GraphPad Prism v10.

559 ***IgM Enzyme Linked Immunosorbent Assay (ELISA)***

560 An ELISA was used to test the interaction between IgM and KE10VAR_R1 domains as previously
561 described (37), with modifications. ELISA plates (Greiner 655061) were coated with 200 µl of 10
562 µg/ml human IgM (Sigma 18260) diluted in 0.1 M carbonate-bicarbonate buffer and incubated at 4°C
563 overnight. Control wells contained buffer but no IgM. After incubation, the coating buffer was
564 flicked off and blocking buffer (PBS/5% skimmed milk/0.1% (v/v) Tween 20) was added for 2 hours at

565 RT. The plate was washed three times with PBS. KE10VAR_R1 DBL proteins were suspended in
566 dilution buffer (PBS/1% skimmed milk/0.1% (v/v) Tween 20) and 150 µl of each DBL protein at four
567 5-fold dilutions (50 µg/ml, 10 µg/ml, 2 µg/ml, 0.4 µg/ml) were added to duplicate wells and
568 incubated overnight at 4°C. After incubation, the plate was washed three times with PBS. 50 µl of
569 anti-His HRP (1:3000) (Biolegend 652404) in dilution buffer was added to each well and incubated at
570 37°C for 1 hour. The plate was washed three times with PBS and twice with deionised water. 50 µl of
571 3,3′,5,5′-Tetramethylbenzidine (TMB) (Sigma, T2885) substrate was added to each well and
572 incubated at RT for 7 mins. The reaction was stopped using 0.18 M sulphuric acid and absorbance
573 read at 450nm. The mean absorbance readings from duplicate wells were plotted against DBL
574 protein concentration using R v4.2.2 (73).

575 ***Host receptor spot binding assays***

576 3 µl spots of recombinant ICAM-1 (50 µg/ml; R&D 720-IC), EPCR (50 µg/ml; Sino Biologicals
577 13320-H02H), CD36 (25 µg/ml; R&D 1955-CD) and PBS, all in duplicate were spotted onto 60 mm
578 diameter bacteriological petri dishes (BD Falcon 351005) and incubated in a humidified chamber
579 overnight at 4°C. Next day the spots were aspirated and 2 ml of PBS/2% BSA blocking buffer was
580 added per dish and incubated for 2 hours at 37°C. During the blocking step, 1.5 ml aliquots of
581 KE08R+ culture suspension at 5-10% parasitemia (predominantly mature pigmented trophozoite
582 stage) and ~2% Ht were prepared by pre-incubation with or without 10 µg/ml of rabbit polyclonal
583 IgG to KE08VAR_R1 NTS-DBLα for 30 mins at 37°C to disrupt rosettes. The blocking solution was
584 removed, dishes washed with incomplete binding medium (IBM, as described above but without
585 serum) and 1.5 ml of the prepared culture suspension was added to each dish. Dishes were
586 incubated at 37°C for 1 hour, with gentle resuspension every 12 minutes. Unbound cells were
587 removed by at least five gentle washes with 4 ml of IBM per wash; bound cells were fixed with
588 PBS/2% glutaraldehyde for at least 30 mins and stained with 5% Giemsa for 10 mins. The number of
589 infected erythrocytes bound to each spot was counted with an inverted microscope using a 40X
590 objective. Technical replicates based on counts of duplicate spots or dishes were averaged to

591 determine a binding value for each receptor in each experiment, and statistical analysis was done on
592 the average binding values from n ≥ 3 independent experiments using one-way ANOVA with
593 Dunnett's multiple comparisons test or two-tailed paired t tests with Holm-Sidak multiple
594 comparisons test. Statistical analyses and graphs were done using GraphPad Prism (Version 10.2.2,
595 GraphPad software, Inc).

596 ***Multiple sequence alignment and motif search***

597 Multiple sequence alignment (MSA) of the NTS-DBLα protein sequences were performed using
598 Clustal Omega, accessible through the European Bioinformatics Institute website
599 (https://www.ebi.ac.uk/Tools/msa/) using default parameters. The MSA output was analysed using
600 Jalview (78) to assess the presence of known rosetting motifs across rosetting and non-rosetting
601 variants. The sequence analysis included NTS-DBLα sequences from experimentally validated
602 PfEMP1 variants, comprising 12 rosetting (Table 2) and 12 non-rosetting (Table 3) variants.

603 **Table 2: *var* genes encode rosetting PfEMP1 variants*.**

S/N	*var* gene/alternative name	Group**	DBLα class	DC	Ref.
1	*pc0053var_r1/9197var15*	A	1.2	15	This study
2	*pfke11var_r1/pfke11.g448*	A	1.2	15	This study
3	*pfke08var_r1/9605.g502*	A	1.8	11	This study
4	*pfke10var_r1/11019var1*	A	1.8	11	This study
5	*IT4var60*	A	1.8	11	(15)
6	*TM284var1*	A	1.8	11	(17)
7	*IT4var09*	A	1.6	16	(14)
8	*PaloAltovarO*	A	1.6	16	(32)
9	*3D7PF13_0003*	A	1.5	16	(16)
10	*HB3var06*	A	1.5	16	(17)
11	*Muz12var1*	A	1.5	16	(17)
12	*TM180var1*	B	2	8	(17)

604 *Parasite lines expressing these variants have been examined microscopically and shown to form rosettes and
605 evidence that the PfEMP1 NTS-DBLa binds erythrocytes has been provided.
606 ** Rask et al (27) or Otto et al (35).
607
608

Table 3: *var* genes encode non-rosetting PfEMP1 variants*.

S/N	*var* gene	Group**	DC	Associated phenotype	Ref.
1	*IT4var19*	B	8	HBEC-binding***	(49)
2	*3D7PFD0020c*	A	8	HBEC-binding	(49)
3	*pfke08var_r1/PFKE08.g501*	B	8	ICAM-1, EPCR	this study
5	*HB3var03*	A	13	HBEC-binding	(49)
6	*IT4var07*	A	13	HBEC-binding	(49)
7	*pc0053-C.g96/9197var5*	B	17	HBEC-binding	Rowe lab unpublished
8	*IT4var44*	B	12	Clumping	Rowe lab unpublished
9	*IT4var67*	B	12	Clumping	Rowe lab unpublished
10	*HB3var05*	A	16	Unknown	Rowe lab unpublished
11	*IT4var14*	B	14	CD36- and ICAM-1 binding	(79)
12	*IT4var16*	B	14	CD36- and ICAM-1 binding	(80)

*Parasite lines expressing these variants have been examined microscopically and no rosettes were seen.
** Rask et al (27) or Otto et al (35).
*** HBEC, human brain endothelial cell

CIDRα1.5 analysis methods

The amino acid sequences of the all PFKE CIDRα1.5 domains were extracted based on previously published domain boundaries (35). The sequences were aligned with default parameters using MUSCLE (v3.8.1551) (81). IQTREE (v2.0.5) was then used to generate a maximum likelihood tree of the aligned sequences (82). The IQTREE command "*iqtree2 --safe -s cidra.aa.aligned.fasta -m JTT+F+I+I+R10 -alrt 1000*" was used and the results were visualised and annotated using ggtree in R (73, 83).

Acknowledgements

This work was funded by the Wellcome Trust grant numbers 084226 (senior fellowship to JAR), 204052/Z/16/Z (PhD studentship to FM), 218492/Z/19/Z (PhD studentship to RL and BRO) and 203077/Z/16/Z (core Award to the KEMRI-Wellcome Trust Research Programme). The work is published with the permission of the Director of KEMRI.

633

634

635

636 **References**

637 1. Lee WC, Russell B, Renia L. Evolving perspectives on rosetting in malaria. Trends Parasitol.
638 2022;38(10):882-9.

639 2. Rowe A, Obeiro J, Newbold CI, Marsh K. *Plasmodium falciparum* rosetting is associated with
640 malaria severity in Kenya. Infect Immun. 1995;63(6):2323-6.

641 3. Carlson J, Helmby H, Hill AV, Brewster D, Greenwood BM, Wahlgren M. Human cerebral
642 malaria: association with erythrocyte rosetting and lack of anti-rosetting antibodies. Lancet.
643 1990;336(8729):1457-60.

644 4. Normark J, Nilsson D, Ribacke U, Winter G, Moll K, Wheelock CE, et al. PfEMP1-DBL1alpha
645 amino acid motifs in severe disease states of *Plasmodium falciparum* malaria. Proc Natl Acad Sci U S
646 A. 2007;104(40):15835-40.

647 5. Doumbo OK, Thera MA, Kone AK, Raza A, Tempest LJ, Lyke KE, et al. High levels of
648 *Plasmodium falciparum* rosetting in all clinical forms of severe malaria in African children. American
649 Journal of Tropical Medicine and Hygiene. 2009;81(6):987-93.

650 6. Nash GB, Cooke BM, Carlson J, Wahlgren M. Rheological properties of rosettes formed by
651 red blood cells parasitized by *Plasmodium falciparum*. Br J Haematol. 1992;82(4):757-63.

652 7. Kaul DK, Roth EFJ, Nagel RL, Howard RJ, Handunnetti SM. Rosetting of *Plasmodium*
653 *falciparum*-infected red blood cells with uninfected red blood cells enhances microvascular
654 obstruction under flow conditions. Blood. 1991;78(3):812-9.

655 8. Chotivanich KT, Dondorp AM, White NJ, Peters K, Vreeken J, Kager PA, et al. The resistance
656 to physiological shear stresses of the erythrocytic rosettes formed by cells infected with *Plasmodium*
657 *falciparum*. Ann Trop Med Parasitol. 2000;94(3):219-26.

658 9. Jotten AM, Moll K, Wahlgren M, Wixforth A, Westerhausen C. Blood group and size
659 dependent stability of *P. falciparum* infected red blood cell aggregates in capillaries.
660 Biomicrofluidics. 2020;14(2):024104.

661 10. Rowe JA, Handel IG, Thera MA, Deans AM, Lyke KE, Koné A, et al. Blood group O protects
662 against severe Plasmodium falciparum malaria through the mechanism of reduced rosetting. Proc
663 Natl Acad Sci U S A. 2007;104(44):17471-6.

664 11. Cockburn IA, Mackinnon MJ, O'Donnell A, Allen SJ, Moulds JM, Baisor M, et al. A human
665 complement receptor 1 polymorphism that reduces *Plasmodium falciparum* rosetting confers
666 protection against severe malaria. Proc Natl Acad Sci U S A. 2004;101(1):272-7.

667 12. Opi DH, Swann O, Macharia A, Uyoga S, Band G, Ndila CM, et al. Two complement receptor
668 one alleles have opposing associations with cerebral malaria and interact with α-thalassaemia. Elife.
669 2018;7.

670 13. Treutiger CJ, Carlson J, Scholander C, Wahlgren M. The time course of cytoadhesion,
671 immunoglobulin binding, rosette formation, and serum-induced agglutination of *Plasmodium*
672 *falciparum*-infected erythrocytes. Am J Trop Med Hyg. 1998;59(2):202-7.
673 14. Rowe JA, Moulds JM, Newbold CI, Miller LH. *P. falciparum* rosetting mediated by a parasite-
674 variant erythrocyte membrane protein and complement-receptor 1. Nature. 1997;388(6639):292-5.
675 15. Albrecht L, Moll K, Blomqvist K, Normark J, Chen Q, Wahlgren M. var gene transcription and
676 PfEMP1 expression in the rosetting and cytoadhesive *Plasmodium falciparum* clone FCR3S1.2. Malar
677 J. 2011;10:17.
678 16. Vigan-Womas I, Guillotte M, Juillerat A, Vallieres C, Lewit-Bentley A, Tall A, et al. Allelic
679 diversity of the *Plasmodium falciparum* erythrocyte membrane protein 1 entails variant-specific red
680 cell surface epitopes. PLoS One. 2011;6(1):e16544.
681 17. Ghumra A, Semblat JP, Ataide R, Kifude C, Adams Y, Claessens A, et al. Induction of strain-
682 transcending antibodies against Group A PfEMP1 surface antigens from virulent malaria parasites.
683 PLoS Pathog. 2012;8(4):e1002665.
684 18. Goel S, Palmkvist M, Moll K, Joannin N, Lara P, Akhouri RR, et al. RIFINs are adhesins
685 implicated in severe *Plasmodium falciparum* malaria. Nature Medicine. 2015;21(4):314-7.
686 19. Niang M, Bei AK, Madnani KG, Pelly S, Dankwa S, Kanjee U, et al. STEVOR is a *Plasmodium*
687 *falciparum* erythrocyte binding protein that mediates merozoite invasion and rosetting. Cell Host
688 Microbe. 2014;16(1):81-93.
689 20. Gardner MJ, Hall N, Fung E, White O, Berriman M, Hyman RW, et al. Genome sequence of
690 the human malaria parasite Plasmodium falciparum. Nature. 2002;419(6906):498-511.
691 21. Kyriacou HM, Stone GN, Challis RJ, Raza A, Lyke KE, Thera MA, et al. Differential var gene
692 transcription in Plasmodium falciparum isolates from patients with cerebral malaria compared to
693 hyperparasitaemia. Molecular and Biochemical Parasitology. 2006;150(2):211-8.
694 22. Lavstsen T, Turner L, Saguti F, Magistrado P, Rask TS, Jespersen JS, et al. Plasmodium
695 falciparum erythrocyte membrane protein 1 domain cassettes 8 and 13 are associated with severe
696 malaria in children. Proc Natl Acad Sci U S A. 2012;109(26):E1791-800.
697 23. Warimwe GM, Fegan G, Musyoki JN, Newton CR, Opiyo M, Githinji G, et al. Prognostic
698 indicators of life-threatening malaria are associated with distinct parasite variant antigen profiles. Sci
699 Transl Med. 2012;4(129):129ra45.
700 24. Bernabeu M, Danziger SA, Avril M, Vaz M, Babar PH, Brazier AJ, et al. Severe adult malaria is
701 associated with specific PfEMP1 adhesion types and high parasite biomass. Proc Natl Acad Sci U S A.
702 2016;113(23):E3270-9.

703 25. Jespersen JS, Wang CW, Mkumbaye SI, Minja DT, Petersen B, Turner L, et al. Plasmodium
704 falciparum var genes expressed in children with severe malaria encode CIDRalpha1 domains. EMBO
705 Mol Med. 2016;8(8):839-50.
706 26. Smith JD, Subramanian G, Gamain B, Baruch DI, Miller LH. Classification of adhesive domains
707 in the *Plasmodium falciparum* erythrocyte membrane protein 1 family. Molecular and Biochemical
708 Parasitology. 2000;110(2):293-310.
709 27. Rask TS, Hansen DA, Theander TG, Gorm Pedersen A, Lavstsen T. *Plasmodium falciparum*
710 erythrocyte membrane protein 1 diversity in seven genomes--divide and conquer. PLoS Comput Biol.
711 2010;6(9):e1000933.
712 28. Smith JD, Rowe JA, Higgins MK, Lavstsen T. Malaria's deadly grip: cytoadhesion of
713 Plasmodium falciparum-infected erythrocytes. Cell Microbiol. 2013;15(12):1976-83.
714 29. Hsieh FL, Turner L, Bolla JR, Robinson CV, Lavstsen T, Higgins MK. The structural basis for
715 CD36 binding by the malaria parasite. Nat Commun. 2016;7:12837.
716 30. Lennartz F, Adams Y, Bengtsson A, Olsen RW, Turner L, Ndam NT, et al. Structure-Guided
717 Identification of a Family of Dual Receptor-Binding PfEMP1 that Is Associated with Cerebral Malaria.
718 Cell Host Microbe. 2017;21(3):403-14.
719 31. Lau CK, Turner L, Jespersen JS, Lowe ED, Petersen B, Wang CW, et al. Structural conservation
720 despite huge sequence diversity allows EPCR binding by the PfEMP1 family implicated in severe
721 childhood malaria. Cell Host Microbe. 2015;17(1):118-29.
722 32. Vigan-Womas I, Guillotte M, Le Scanf C, Igonet S, Petres S, Juillerat A, et al. An in vivo and in
723 vitro model of *Plasmodium falciparum* rosetting and autoagglutination mediated by varO, a group A
724 var gene encoding a frequent serotype. Infect Immun. 2008;76(12):5565-80.
725 33. Tan J, Pieper K, Piccoli L, Abdi A, Perez MF, Geiger R, et al. A LAIR1 insertion generates
726 broadly reactive antibodies against malaria variant antigens. Nature. 2016;529(7584):105-9.
727 34. Kioko M, Pance A, Mwangi S, Goulding D, Kemp A, Rono M, et al. Extracellular vesicles could
728 be a putative posttranscriptional regulatory mechanism that shapes intracellular RNA levels in
729 Plasmodium falciparum. Nat Commun. 2023;14(1):6447.
730 35. Otto TD, Assefa SA, Bohme U, Sanders MJ, Kwiatkowski D, Pf3k c, et al. Evolutionary analysis
731 of the most polymorphic gene family in falciparum malaria. Wellcome Open Res. 2019;4:193.
732 36. Peters JM, Fowler EV, Krause DR, Cheng Q, Gatton ML. Differential changes in *Plasmodium*
733 *falciparum var* transcription during adaptation to culture. J Infect Dis. 2007;195(5):748-55.
734 37. Ghumra A, Semblat JP, McIntosh RS, Raza A, Rasmussen IB, Braathen R, et al. Identification
735 of residues in the Cmu4 domain of polymeric IgM essential for interaction with *Plasmodium*

736 *falciparum* erythrocyte membrane protein 1 (PfEMP1). Journal of Immunology. 2008;181(3):1988-
737 2000.
738 38. Stevenson L, Huda P, Jeppesen A, Laursen E, Rowe JA, Craig A, et al. Investigating the
739 function of F -specific binding of IgM to *Plasmodium falciparum* erythrocyte membrane protein 1
740 mediating erythrocyte rosetting. Cell Microbiol. 2014.
741 39. Akhouri RR, Goel S, Furusho H, Skoglund U, Wahlgren M. Architecture of Human IgM in
742 Complex with *P. falciparum* Erythrocyte Membrane Protein 1. Cell Rep. 2016;14(4):723-36.
743 40. Heddini A, Pettersson F, Kai O, Shafi J, Obiero J, Chen Q, et al. Fresh isolates from children
744 with severe Plasmodium falciparum malaria bind to multiple receptors. Infect Immun.
745 2001;69(9):5849-56.
746 41. Rowe JA, Shafi J, Kai OK, Marsh K, Raza A. Nonimmune IgM, but not IgG binds to the surface
747 of *Plasmodium falciparum*-infected erythrocytes and correlates with rosetting and severe malaria.
748 American Journal of Tropical Medicine and Hygiene. 2002;66(6):692-9.
749 42. Stevenson L, Laursen E, Cowan GJ, Bandoh B, Barfod L, Cavanagh DR, et al. α2-Macroglobulin
750 Can Crosslink Multiple *Plasmodium falciparum* Erythrocyte Membrane Protein 1 (PfEMP1) Molecules
751 and May Facilitate Adhesion of Parasitized Erythrocytes. PLoS Pathog. 2015;11(7):e1005022.
752 43. Leech JH, Barnwell JW, Miller LH, Howard RJ. Identification of a strain-specific malarial
753 antigen exposed on the surface of *Plasmodium falciparum* infected erythrocytes. J Exp Med.
754 1984;159:1567-75.
755 44. Kyes SA, Rowe JA, Kriek N, Newbold CI. Rifins: a second family of clonally variant proteins
756 expressed on the surface of red cells infected with *Plasmodium falciparum*. Proc Natl Acad Sci U S A.
757 1999;96(16):9333-8.
758 45. Fernandez V, Hommel M, Chen Q, Hagblom P, Wahlgren M. Small, clonally variant antigens
759 expressed on the surface of the *Plasmodium falciparum*-infected erythrocyte are encoded by the rif
760 gene family and are the target of human immune responses. J Exp Med. 1999;190(10):1393-404.
761 46. Bull PC, Berriman M, Kyes S, Quail MA, Hall N, Kortok MM, et al. *Plasmodium falciparum*
762 Variant Surface Antigen Expression Patterns during Malaria. PLoS Pathog. 2005;1(3):e26.
763 47. Turner L, Lavstsen T, Berger SS, Wang CW, Petersen JE, Avril M, et al. Severe malaria is
764 associated with parasite binding to endothelial protein C receptor. Nature. 2013;498(7455):502-5.
765 48. Ghumra A, Khunrae P, Ataide R, Raza A, Rogerson SJ, Higgins MK, et al. Immunisation with
766 recombinant PfEMP1 domains elicits functional rosette-inhibiting and phagocytosis-inducing
767 antibodies to *Plasmodium falciparum*. PLoS One. 2011;6(1):e16414.

768 49. Claessens A, Adams Y, Ghumra A, Lindergard G, Buchan CC, Andisi C, et al. A subset of group
769 A-like *var* genes encodes the malaria parasite ligands for binding to human brain endothelial cells.
770 Proc Natl Acad Sci U S A. 2012;109:E1772-81.
771 50. Voss TS, Healer J, Marty AJ, Duffy MF, Thompson JK, Beeson JG, et al. A var gene promoter
772 controls allelic exclusion of virulence genes in Plasmodium falciparum malaria. Nature.
773 2006;439(7079):1004-8.
774 51. Joergensen L, Bengtsson DC, Bengtsson A, Ronander E, Berger SS, Turner L, et al. Surface co-
775 expression of two different PfEMP1 antigens on single plasmodium falciparum-infected erythrocytes
776 facilitates binding to ICAM1 and PECAM1. PLoS Pathog. 2010;6(9):e1001083.
777 52. Vigan-Womas I, Guillotte M, Juillerat A, Hessel A, Raynal B, England P, et al. Structural basis
778 for the ABO blood-group dependence of *Plasmodium falciparum* rosetting. PLoS Pathog.
779 2012;8(7):e1002781.
780 53. Ji C, Shen H, Su C, Li Y, Chen S, Sharp TH, et al. Plasmodium falciparum has evolved multiple
781 mechanisms to hijack human immunoglobulin M. Nat Commun. 2023;14(1):2650.
782 54. Handunnetti SM, Hasler TH, Howard RJ. *Plasmodium falciparum*-infected erythrocytes do
783 not adhere well to C32 melanoma cells or CD36 unless rosettes with uninfected erythrocytes are
784 first disrupted. Infect Immun. 1992;60(3):928-32.
785 55. Rorick MM, Baskerville EB, Rask TS, Day KP, Pascual M. Identifying functional groups among
786 the diverse, recombining antigenic var genes of the malaria parasite Plasmodium falciparum from a
787 local community in Ghana. PLoS Comput Biol. 2018;14(6):e1006174.
788 56. McQuaid F, Rowe JA. Rosetting revisited: a critical look at the evidence for host erythrocyte
789 receptors in Plasmodium falciparum rosetting. Parasitology. 2020;147(1):1-11.
790 57. Deb B, Das A, Vilvadrinath R, Jangra A, Shukla MS, Akhouri RR, et al. Glycophorin B-PfEMP1
791 interaction mediates robust rosetting in Plasmodium falciparum. Int J Biol Macromol. 2024;262(Pt
792 1):129868.
793 58. Le Scanf C, Vigan-Womas I, Contamin H, Guillotte M, Bischoff E, Mercereau-Puijalon O.
794 Rosetting is associated with increased Plasmodium falciparum in vivo multiplication rate in the
795 Saimiri sciureus monkey. Microbes Infect. 2008;10(4):447-51.
796 59. Mackinnon MJ, Read AF. Genetic relationships between parasite virulence and transmission
797 in the rodent malaria *Plasmodium chabaudi*. Evolution. 1999;54:689-703.
798 60. Clough B, Atilola FA, Pasvol G. The role of rosetting in the multiplication of *Plasmodium*
799 *falciparum*: rosette formation neither enhances nor targets parasite invasion into uninfected red
800 cells. Brit J Haematol. 1998;100(1):99-104.

801 61. Deans AM, Rowe JA. Plasmodium falciparum: Rosettes do not protect merozoites from
802 invasion-inhibitory antibodies. Experimental Parasitol. 2006;112(4):269-73.
803 62. Moll K, Palmkvist M, Ch'ng J, Kiwuwa MS, Wahlgren M. Evasion of Immunity to Plasmodium
804 falciparum: Rosettes of Blood Group A Impair Recognition of PfEMP1. PLoS One.
805 2015;10(12):e0145120.
806 63. Magallon-Tejada A, Machevo S, Cistero P, Lavstsen T, Aide P, Rubio M, et al. Cytoadhesion to
807 gC1qR through Plasmodium falciparum Erythrocyte Membrane Protein 1 in Severe Malaria. PLoS
808 Pathog. 2016;12(11):e1006011.
809 64. Wichers JS, Tonkin-Hill G, Thye T, Krumkamp R, Kreuels B, Strauss J, et al. Common virulence
810 gene expression in adult first-time infected malaria patients and severe cases. Elife. 2021;10.
811 65. Dondorp AM, Pongponratn E, White NJ. Reduced microcirculatory flow in severe falciparum
812 malaria: pathophysiology and electron-microscopic pathology. Acta Trop. 2004;89(3):309-17.
813 66. Barrera V, MacCormick IJC, Czanner G, Hiscott PS, White VA, Craig AG, et al. Neurovascular
814 sequestration in paediatric P. falciparum malaria is visible clinically in the retina. Elife. 2018;7.
815 67. Ben Abderrahim S, Gharsallaoui S, Ben Daly A, Mosbahi A, Chaieb S, Nfikha Z, et al. Imported
816 malaria in adults: about a case of cerebral malaria. Egypt J Forensic Sci. 2022;12(1):19.
817 68. Vogt AM, Barragan A, Chen Q, Kironde F, Spillmann D, Wahlgren M. Heparan sulfate on
818 endothelial cells mediates the binding of Plasmodium falciparum-infected erythrocytes via the
819 DBL1alpha domain of PfEMP1. Blood. 2003;101(6):2405-11.
820 69. Adams Y, Kuhnrae P, Higgins MK, Ghumra A, Rowe JA. Rosetting *Plasmodium falciparum*-
821 infected erythrocytes bind to human brain microvascular endothelial cells in vitro, demonstrating a
822 dual adhesion phenotype mediated by distinct *P. falciparum* erythrocyte membrane protein 1
823 domains. Infect Immun. 2014;82(3):949-59.
824 70. Scherf A, Hernandez-Rivas R, Buffet P, Bottius E, Benatar C, Pouvelle B, et al. Antigenic
825 variation in malaria: in situ switching, relaxed and mutually exclusive transcription of var genes
826 during intra-erythrocytic development in Plasmodium falciparum. EMBO J. 1998;17(18):5418-26.
827 71. McLean FE, Azasi Y, Sutherland C, Toboh E, Ansong D, Agbenyega T, et al. Detection of
828 naturally acquired, strain-transcending antibodies against rosetting Plasmodium falciparum strains in
829 humans. Infect Immun. 2024:e0001524.
830 72. Handunnetti SM, Gilladoga AD, van Schravendijk MR, Nakamura K, Aikawa M, Howard RJ.
831 Purification and in vitro selection of rosette-positive (R+) and rosette-negative (R-) phenotypes of
832 knob-positive *Plasmodium falciparum* parasites. Am J Trop Med Hyg. 1992;46(4):371-81.
833 73. R Core Team. R: A Language and Environment for Statistical Computing. R Foundation for
834 Statistical Computing; 2022.

835 74. Altschul SF, Gish W, Miller W, Myers EW, Lipman DJ. Basic local alignment search tool. J Mol
836 Biol. 1990;215(3):403-10.
837 75. Kraemer SM, Gupta L, Smith JD. New tools to identify var sequence tags and clone full-length
838 genes using type-specific primers to Duffy binding-like domains. Mol Biochem Parasitol.
839 2003;129(1):91-102.
840 76. Higgins MK. Overproduction, purification and crystallization of a chondroitin sulfate A-
841 binding DBL domain from a Plasmodium falciparum var2csa-encoded PfEMP1 protein. Acta
842 Crystallogr Sect F Struct Biol Cryst Commun. 2008;64(Pt 3):221-3.
843 77. Angeletti D, Sandalova T, Wahlgren M, Achour A. Binding of subdomains 1/2 of PfEMP1-
844 DBL1alpha to heparan sulfate or heparin mediates Plasmodium falciparum rosetting. PLoS One.
845 2015;10(3):e0118898.
846 78. Waterhouse AM, Procter JB, Martin DM, Clamp M, Barton GJ. Jalview Version 2--a multiple
847 sequence alignment editor and analysis workbench. Bioinformatics. 2009;25(9):1189-91.
848 79. Janes JH, Wang CP, Levin-Edens E, Vigan-Womas I, Guillotte M, Melcher M, et al.
849 Investigating the Host Binding Signature on the Plasmodium falciparum PfEMP1 Protein Family. PLoS
850 Pathog. 2011;7(5):e1002032.
851 80. Avril M, Tripathi AK, Brazier AJ, Andisi C, Janes JH, Soma VL, et al. A restricted subset of var
852 genes mediates adherence of Plasmodium falciparum-infected erythrocytes to brain endothelial
853 cells. Proc Natl Acad Sci U S A. 2012;109(26):E1782-90.
854 81. Edgar RC. MUSCLE: multiple sequence alignment with high accuracy and high throughput.
855 Nucleic Acids Res. 2004;32(5):1792-7.
856 82. Nguyen LT, Schmidt HA, von Haeseler A, Minh BQ. IQ-TREE: a fast and effective stochastic
857 algorithm for estimating maximum-likelihood phylogenies. Mol Biol Evol. 2015;32(1):268-74.
858 83. Yu G, Smith DK, Zhu H, Guan Y, Lam TT-Y. ggtree: an r package for visualization and
859 annotation of phylogenetic trees with their covariates and other associated data. Methods Ecol
860 Evol. 2017;8(1):28-36.
861

862

863 **A**

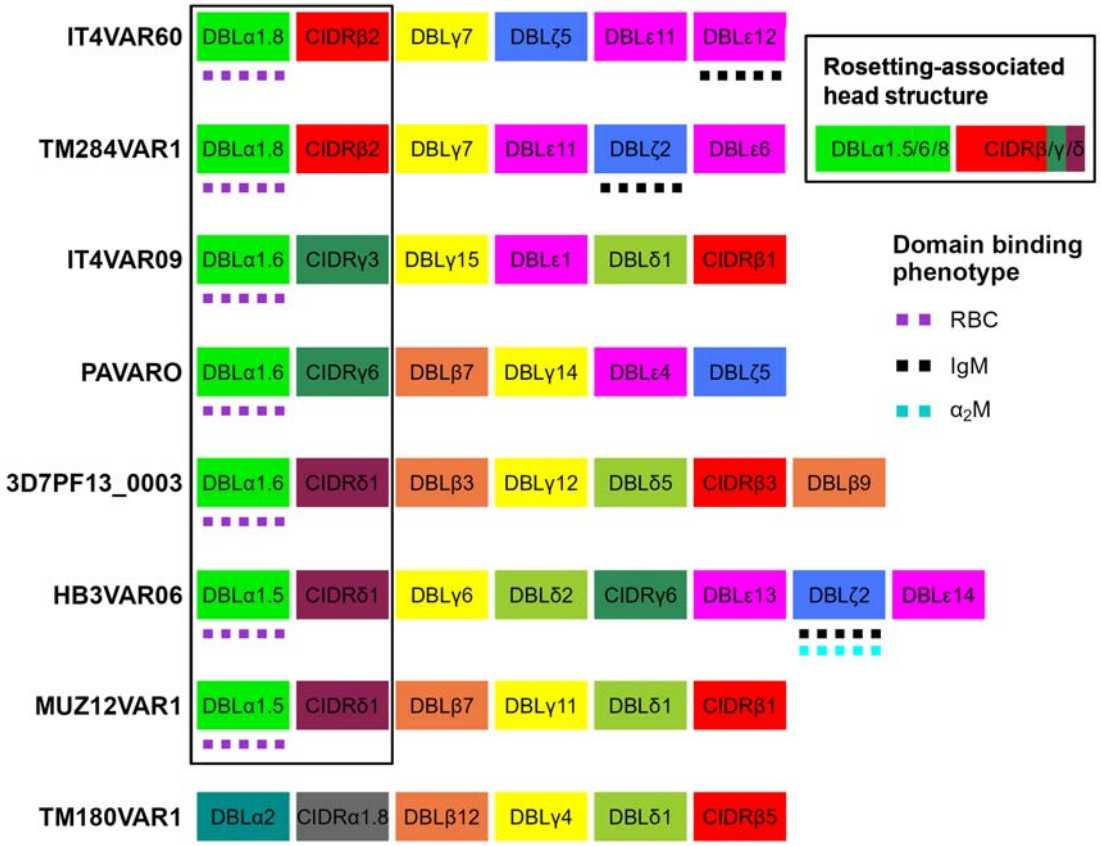

864

865 **B**

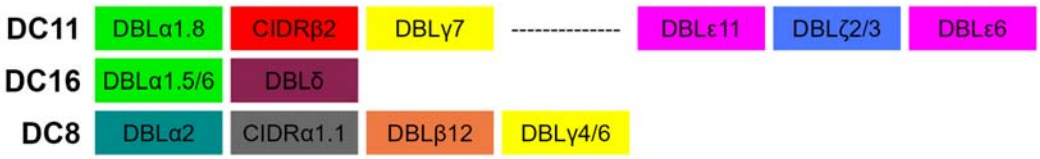

866
867
868
869 **Figure 1. Known rosette-mediating PfEMP1 variants and associated domain cassettes.** A) Diagram
870 of the PfEMP1 domain architecture of known rosette-mediating variants (14-17). The rosetting-
871 associated head structure, DBLα1.5/6/8-CIDRβ/γ/δ, is boxed. Domains that bind erythrocytes (RBC)
872 or serum proteins (IgM and α2M) are indicated. **B)** Diagram of domain cassettes (DCs) [as described
873 by (27)] which are relevant to the rosetting PfEMP1 variants characterised previously.

874
875
876

877 **A**

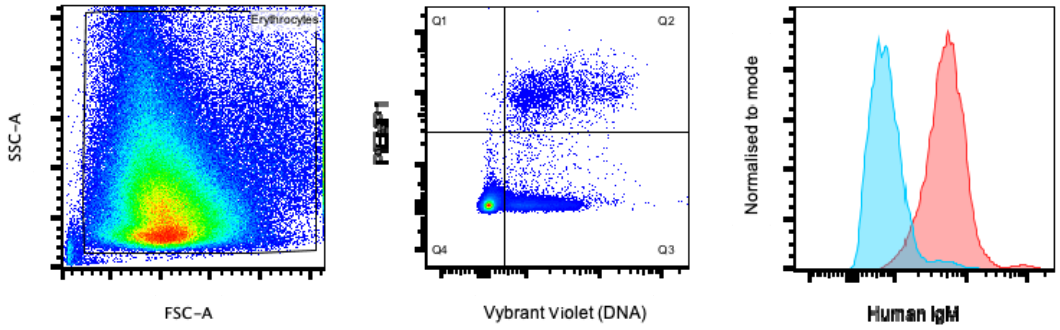

878

879 **B**

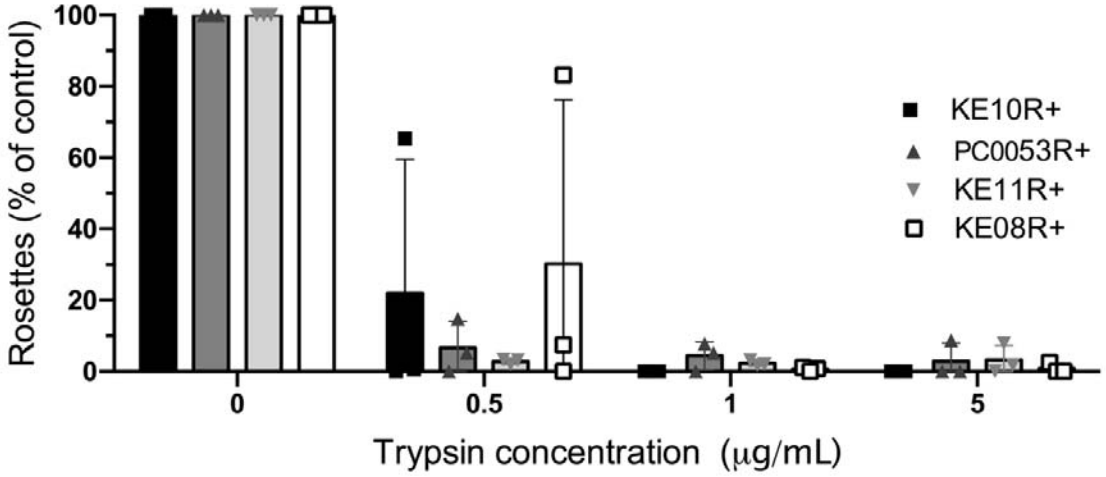

880
881

882 **Figure 2. Properties of the new Kenyan rosetting lines.** A) IgM binding by KE10R+ infected
883 erythrocytes detected by flow cytometry. Forward and side scatter were used to gate on
884 erythrocytes and exclude debris (left panel) and KE10VAR_R1-expressing infected erythrocytes were
885 detected by staining with 20μg/ml of polyclonal rabbit IgG against NTS-DBLα followed by 1/1000
886 dilution of Alexa Fluor 647-conjugated goat anti-rabbit IgG secondary antibody and 1/2500 dilution
887 of Vybrant DyeCycle Violet (middle panel Q2). IgM staining of the Q2 cell population was detected
888 with 1/1000 dilution of an Alexa Fluor 488-conjugated goat anti-human IgM heavy chain antibody
889 (red). The negative control (blue) was parasites grown in IgM-depleted medium and stained with the
890 same antibodies. Results are representative of two independent experiments. B) Effect of low-dose
891 trypsinisation on rosetting. Purified infected erythrocytes were treated with 0.5, 1 or 5 μg/ml of
892 trypsin for 5 mins and the rosette frequency relative to a control sample with no added enzyme was
893 calculated. The mean and standard deviation from three independent experiments per parasite line
894 is shown. The rosette frequency of the untreated controls was between 46%-81% (KE10R+), 45%-
895 89% (PC0053R+), 16%-30% (KE11R+) and 61%-91% (KE08R+).

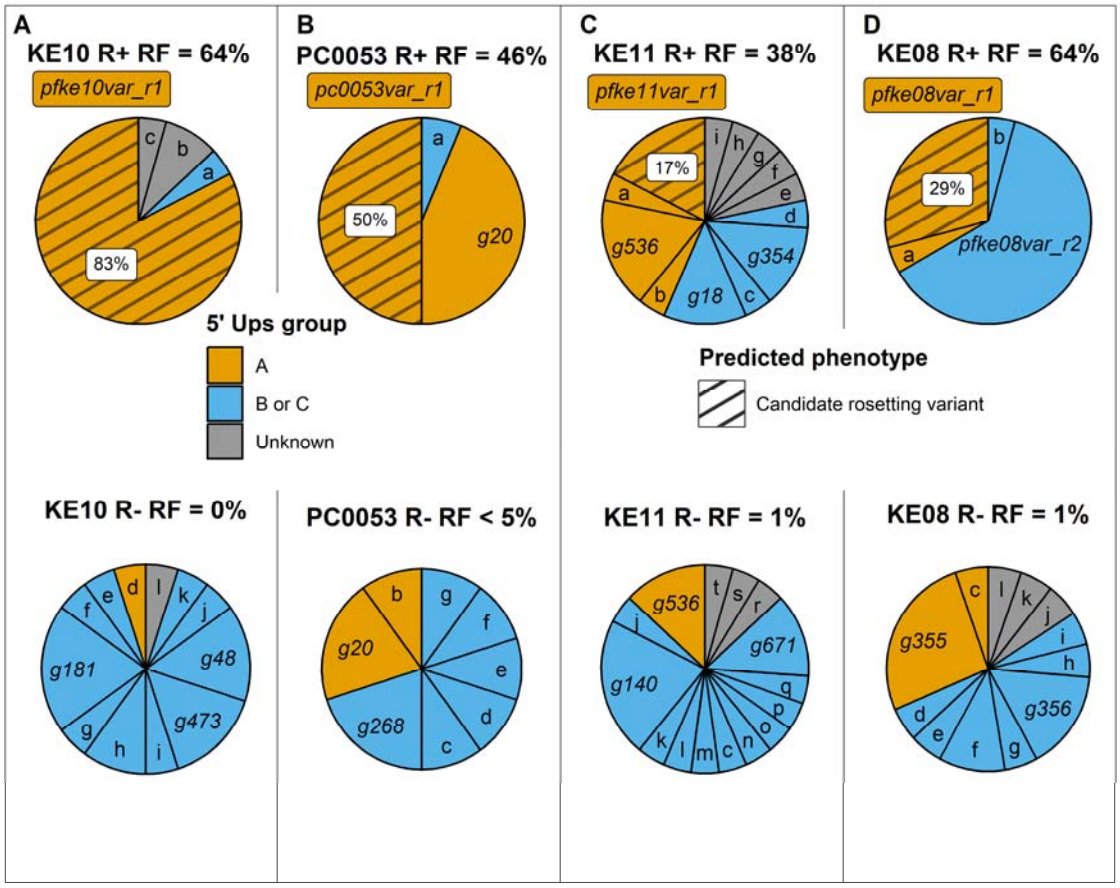

Figure 3. DBLα expression tag profiling of the new Kenyan rosetting lines. DBLα tag expression profiles showing the proportion each gene tag contributed to the overall expressed tag profile for each parasite population. *var* gene tags encoding candidate rosetting variants (hatched; percentage of all tags given in white box) are identified as predominant genes expressed in R+ parasites but not/rarely in isogenic R- parasites. Other large pie slices are identified by gene (g) number for each parasite line, and small slices are given letters, with the full information for each gene given in Supplementary Table 1. *var* gene groups are identified by colour. Slices labelled as "unknown" are from sequence tags that did not map back to an assembled *var* gene in that parasite's repertoire (34). The rosette frequency (RF) in the cycle in which the RNA was collected is shown for each parasite line. Results are representative of two independent experiments.

Figure 4. Domain architecture of the candidate rosette-mediating PfEMP1 variants. Domain cassettes are as described by Rask et al (27). The alternative names for these genes in the Pf3k database (34) are as follows: *pfke10var_r1/PX0203.g54; pc0053var_r1/PC0053-C.g687; pfke11var_r1/ PFKE11.g448 ; pfke08var_r1/ PFKE08.g502; pfke08var_r2/ PFKE08.g501.*

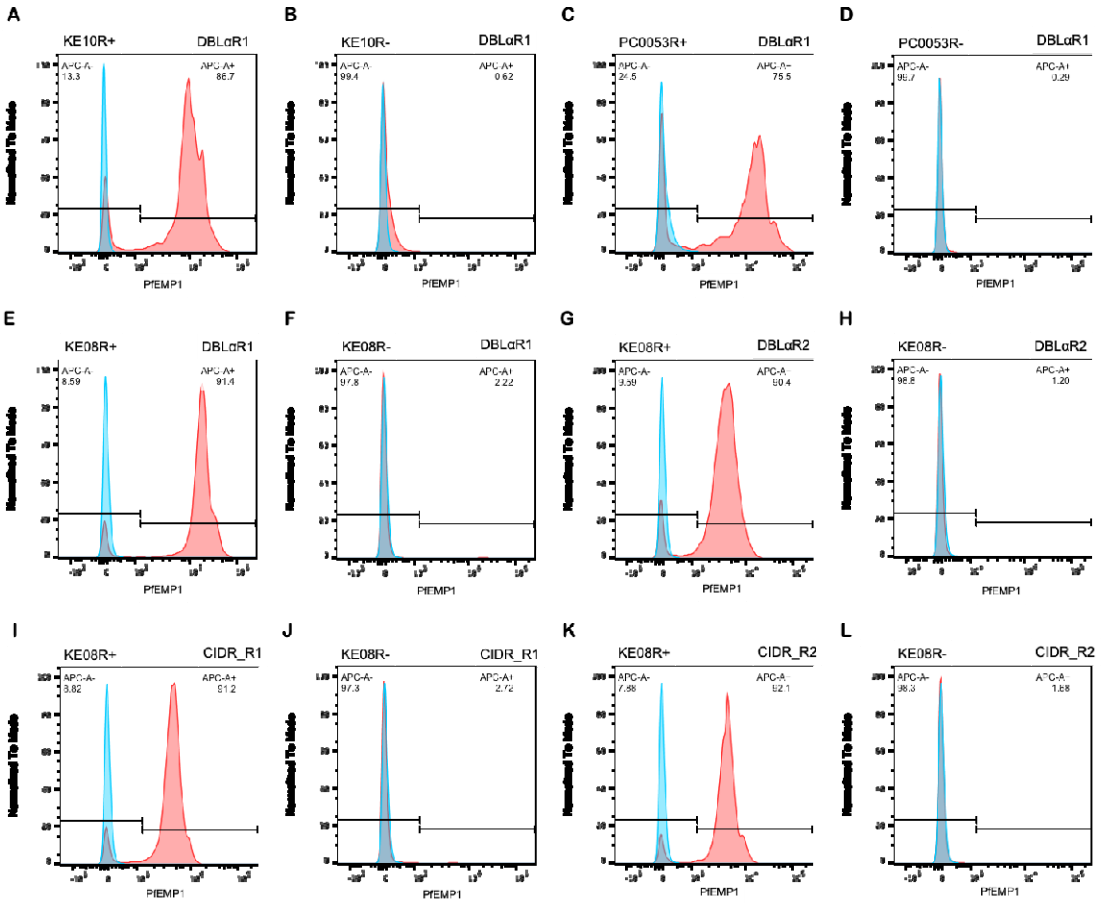

Figure 5. Staining of the surface of live infected erythrocytes with PfEMP1 antibodies. Fluorescence intensity histograms of rosetting (R+) and non-rosetting (R-) parasite lines stained with rabbit IgG against rosetting PfEMP1 variants (red) or negative control rabbit IgG against the NTS-DBLα domain of an irrelevant PfEMP1 variant (HB3VAR03, blue). A) parasite line KE10R+ with antibodies to KE10VAR_R1 NTS-DBLα. B) parasite line KE10R- with antibodies to KE10VAR_R1 NTS-DBLα. C) parasite line PC0053R+ with antibodies to PC0053VAR_R1 NTS-DBLα. D) parasite line PC0053R- with antibodies to PC0053VAR_R1 NTS-DBLα. E) parasite line KE08R+ with antibodies to KE08VAR_R1 NTS-DBLα. F) parasite line KE08R- with antibodies to KE08VAR_R1 NTS-DBLα. G) parasite line KE08R+ with antibodies to KE08VAR_R2 NTS-DBLα. H) parasite line KE08R- with antibodies to KE08VAR_R2 NTS-DBLα. I) parasite line KE08R+ with antibodies to KE08VAR_R1 CIDR. J) parasite line KE08R- with antibodies to KE08VAR_R1 CIDR. K) parasite line KE08R+ with antibodies to KE08VAR_R3 CIDR. L) parasite line KE08R- with antibodies to KE08VAR_R2 CIDR. PfEMP1 was detected with 20µg/ml rabbit IgG against PfEMP1 and 1/1000 dilution of Alexa Fluor 647-conjugated goat anti-rabbit IgG secondary antibody. Gates shows the percentage of mature infected erythrocytes positive for the variant. The rosette frequency at the time of staining was 70-90% for the R+ lines and <2% for the R- lines, and the percentage of positive staining infected erythrocytes

959 (APC-A+, top right corner of each histogram) closely matched the rosette frequency in each parasite
960 line. Results are representative of at least two experiments for each parasite line.
961

962

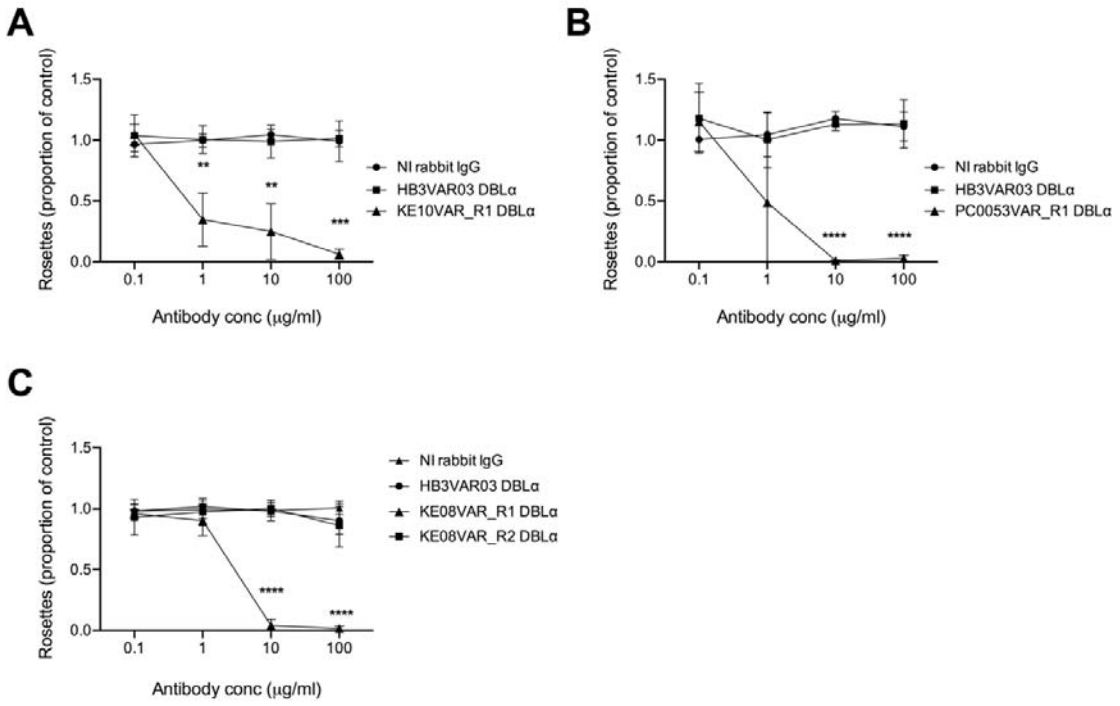

963
964

965 **Figure 6. Rosette disruption with rabbit IgG raised against candidate rosetting PfEMP1 variants.**
966 Antibodies to the candidate rosette-mediating PfEMP1 variant NTS-DBLα domains were tested in
967 rosette-disruption assays over a range of concentrations from 0.1-100 μg/mL. The rosette frequency
968 in the presence of antibody is shown as the proportion of the control value with no added antibody.
969 IgG from a non-immunised (NI) rabbit and from a rabbit immunised with the NTS-DBLα domain of a
970 non-rosetting PfEMP1 variant HB3VAR03 were used as negative controls in all experiments. Data
971 represent three independent experiments with the mean and standard deviation of the three
972 experiments shown. A) parasite line KE10R+; the rosette frequency of the no antibody control
973 ranged from 71%-87%. B) Parasite line PC0053R+; the rosette frequency of the no antibody control
974 ranged from 49%-60%. C) Parasite line KE08R+; the rosette frequency of the no antibody control
975 ranged from 69%-92%. Data were analyzed by two-tailed paired t tests corrected for multiple
976 comparisons with the Holm-Sidak method ** $P<0.01$, *** $P<0.001$, **** $P<0.0001$.

977
978

979 **A**

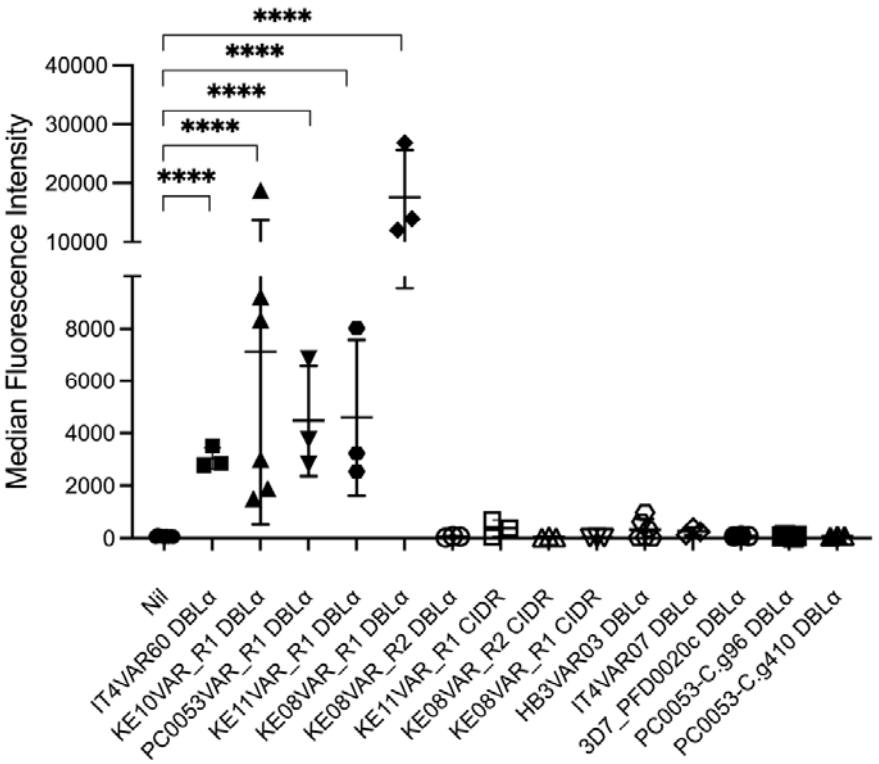

980

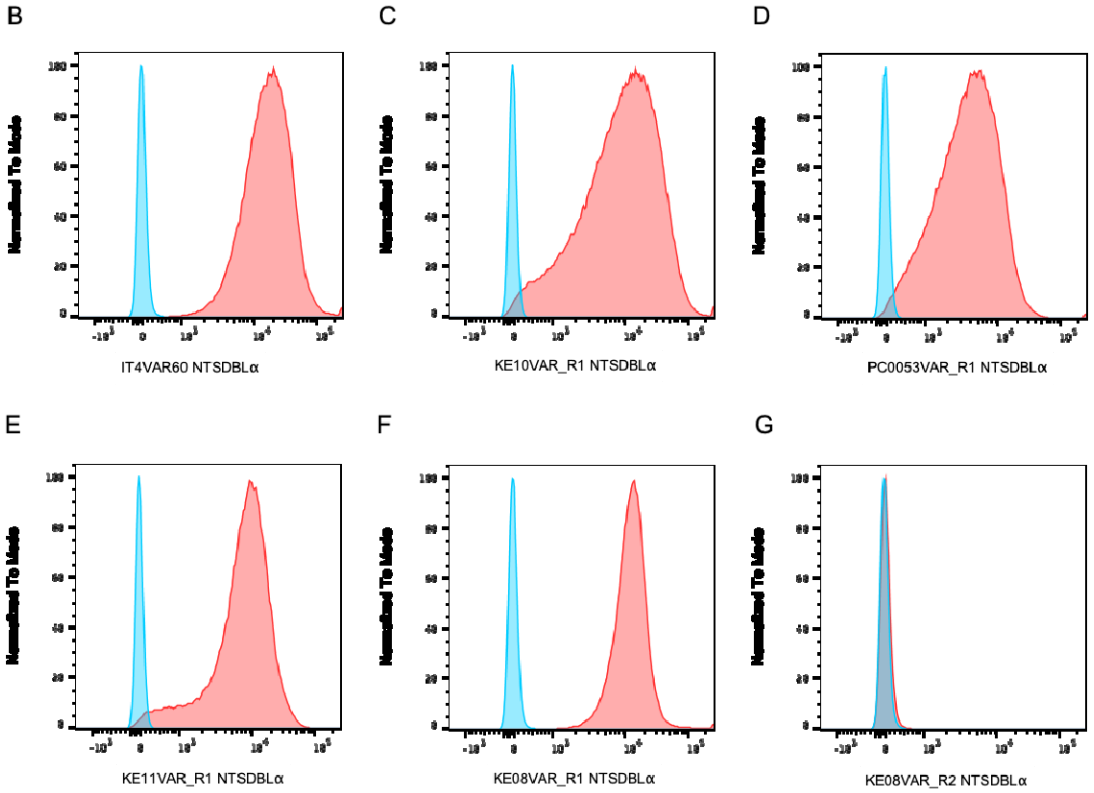

981

982 **Figure 7. Binding of PfEMP1 recombinant proteins to erythrocytes.** A) Recombinant proteins were

983 incubated with uninfected erythrocytes and bound protein detected with specific antibodies to each

984 domain. The positive control was the NTS-DBLα domain of the well-characterised rosetting variant
985 IT4var60 (15, 17) and negative controls were the NTS-DBLα domains from human brain endothelial
986 cell binding PfEMP1 variants HB3VAR03 (PFHB3_130080100), IT4VAR07 (PFIT_060036700),
987 3D7_PFD0020c (PF3D7_0400400), PC0053-C.g96 and PC0053-C.g410 that are known to be non-
988 rosetting (reference 48) and JA Rowe unpublished data). The mean and standard deviation of the
989 Alexa Fluor 488 median fluorescence intensity from at least three independent experiments per
990 protein is indicated. Data were log transformed and analysed by one way ANOVA with Dunnett's
991 multiple comparisons test compared to the "Nil" (no added protein) control. **** P<0.0001. B-G)
992 Example Alexa Fluor 488 fluorescence intensity histograms of recombinant PfEMP1 domains bound
993 to erythrocytes and detected by indirect immunofluorescence (red) compared to a non-rosetting
994 NTS-DBLα domain negative control (blue). The domain tested is indicated below each histogram.
995
996
997

998
999
1000
1001
1002

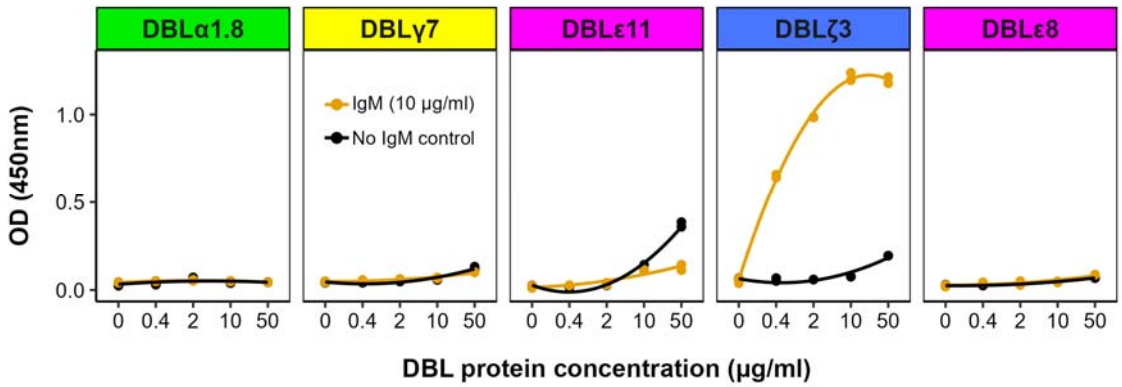

1003
1004
1005

1006 **Figure 8**. **The DBLζ3 domain of PFKE10VAR_R1 binds human IgM.** IgM was coated onto the wells of
1007 an ELISA plate and individual PfEMP1 recombinant protein domains were added at four different 5-
1008 fold dilutions. Wells with no IgM were included as negative controls. Binding was detected using an
1009 HRP-conjugated anti-his tag antibody with TMB substrate and the absorbance read at 450nm. The
1010 domains are shown from N- to C-terminal and the panels are colour-coded as previously described
1011 (27). One representative experiment is shown out of at least two performed for each domain.
1012

1013

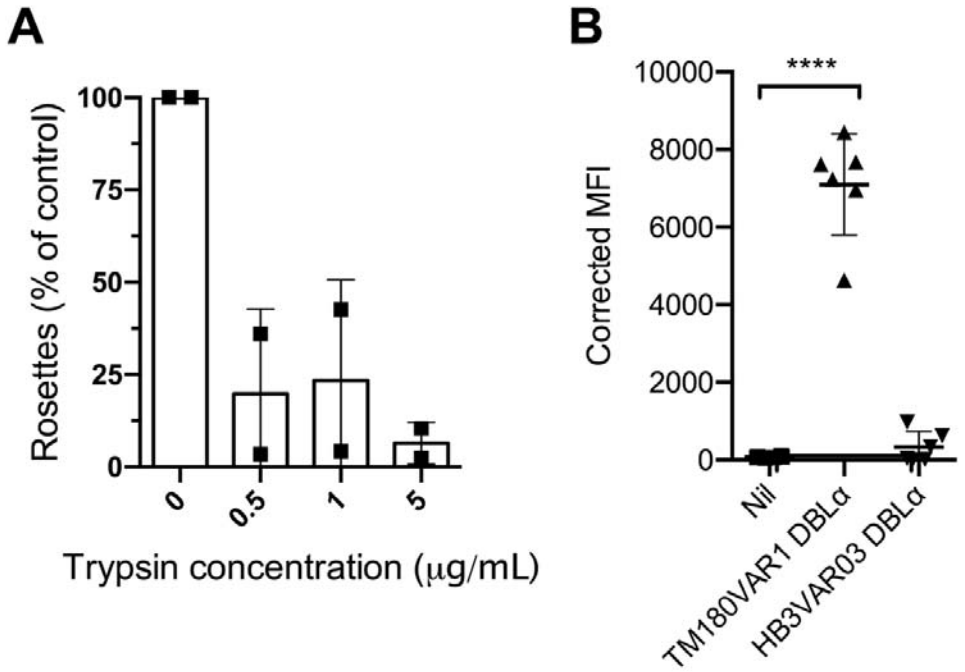

1014
1015

1016 **Figure 9. The NTS-DBLα domain of TM180VAR1 mediates rosetting.** A) Effect of low dose
1017 trypsinisation on TM180R^{+}. Infected erythrocytes were treated with 0.5, 1 or 5 μg/ml of trypsin for 5
1018 mins in each experiment and the rosette frequency relative to a control sample with no added
1019 enzyme was calculated**.** Data represent two independent experiments with the mean indicated by
1020 bar height and the standard deviation shown. The rosette frequency in the untreated controls were
1021 72% and 61% respectively. B) Corrected Median Fluorescence Intensities (MFI) of uninfected
1022 erythrocytes in binding experiments with recombinant TM180VAR1 NTS-DBLα and the negative
1023 control HB3VAR03 NTS-DBLα compared to "Nil" no added protein control. Data are from six
1024 independent experiments and the mean and standard deviation are shown. Significant differences
1025 by one-way ANOVA with Dunnett's multiple comparisons test compared to the "Nil" negative
1026 control are indicated. ****P<0.0001.

1027
1028
1029
1030
1031
1032
1033
1034
1035
1036
1037

1038
1039
1040
1041

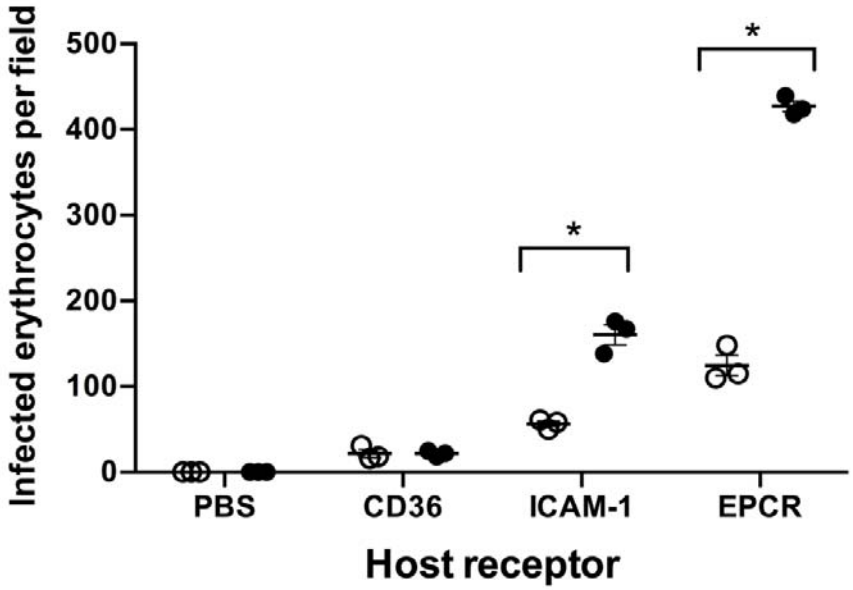

1042
1043
1044
1045 **Figure 10. Spot binding assay of KE08R+ to endothelial cell receptor proteins.** Adhesion of KE08R+
1046 infected erythrocytes to recombinant host receptor proteins was determined with (black circles) and
1047 without (white circles) prior rosette disruption with antibodies to KE08VAR_R1 NTS-DBLα. The
1048 number of infected erythrocytes bound per field was determined using an inverted microscope with
1049 a 40X objective and six fields were counted per spot in each experiment. The difference in mean
1050 binding values compared with the same receptor in the presence and absence of rosette from n=3
1051 independent experiments was analyzed by two-tailed paired t tests corrected for multiple
1052 comparisons with the Holm-Sidak method. *P< 0.05.

1053
1054
1055

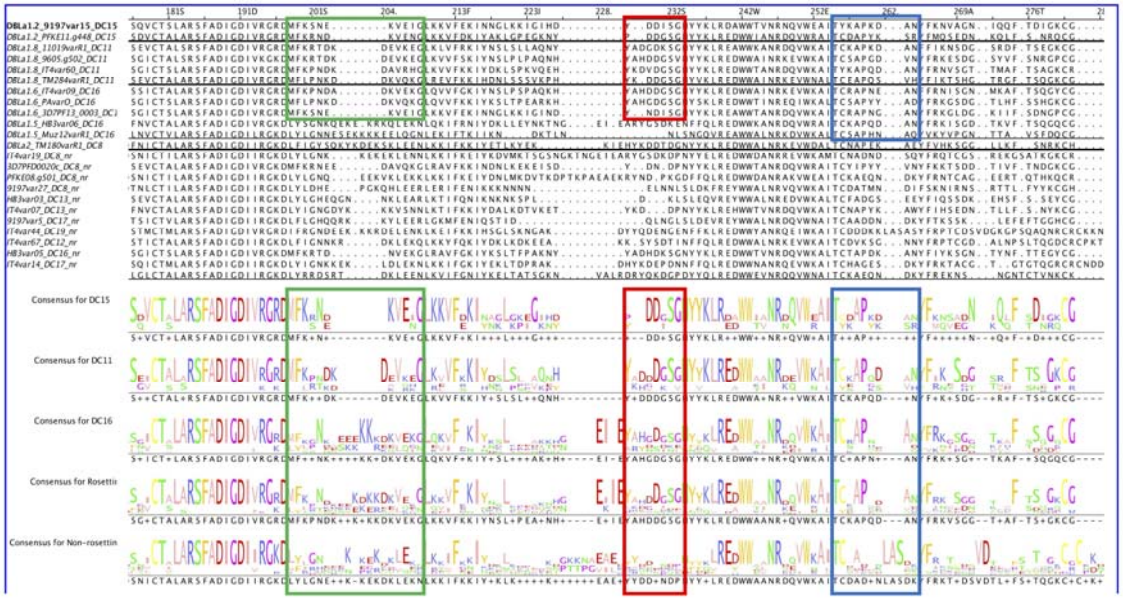

Figure 11. Rosetting motifs. The NTS-DBLα amino acid sequences from known rosetting (upper) and non-rosetting (lower) sequences were aligned in Jalview and amino acid motifs over-represented in the rosetting variants are shown in green, red and blue boxes.